Thermal/Hydraulic Analysis Research Program Quarterly Report October–December 1983

S. L. Thompson, Person in Charge

Prepared for
U. S. NUCLEAR REGULATORY COMMISSION

SF 2900-Q(6-82)

NUREG/CR-3329 Vol. 4 of 4
SAND83-1171
R-4

THERMAL/HYDRAULIC ANALYSIS RESEARCH PROGRAM
QUARTERLY REPORT OCTOBER-DECEMBER 1983

S. L. Thompson, Person in Charge

Date Published: March 1984

DA Dahlgren
Manager, Reactor Systems Test and Analysis Department

C. Upha Lueyeler
Director, Nuclear Fuel Cycle Programs

Sandia National Laboratories
Albuquerque, NM 87185
Operated by
Sandia Corporation
U. S. Department of Energy

LIST OF CONTRIBUTORS

Lawrence D. Buxton

Dean Dobranich

Mildred G. Elrick

Lubomyra Nadia Kmetyk

Andrew C. Peterson

TABLE OF CONTENTS

LIST OF FIGURES

LIST OF TABLES

SUMMARY STATUS REPORT

The TRAC-PF1/MOD1 independent assessment program at Sandia
National Laboratories (SNLA) is part of a multi-faceted effort
sponsored by the Nuclear Regulatory Commission (NRC) to determine
the ability of various systems codes to predict the detailed
thermal/hydraulic response of LWRs during accident and off-normal
conditions. This program is a successor to the RELAP5/MOD1 inde-
pendent assessment project underway at Sandia for the last two
years.

The TRAC-PF1/MOD1 code [1] will be assessed against data from
various integral and separate effects experimental test facilities,
and the calculated results will also be compared with results from
our previous RELAP5/MOD1 independent assessment analyses whenever
possible.

The first quarter of FY84 marks the beginning of the
TRAC-PF1/MOD1 independent assessment project at SNLA. The code was
obtained from Los Alamos National Laboratory (LANL) in October,
and brought up on both our Cyber-76 and Cray-1S computers. The
assessment matrix was formalized, several TRAC nodalizations for
the various facilities required have been developed, and limited
calculations were begun during this quarter.

At the request of the NRC contract monitor, the FY83 and FY84
assessment programs at SNLA were expanded to include a TRAC-PF1
noding study for a design-basis 200% cold leg break accident for
the Sequoyah UHI plant. A fine-node analysis had been done previ-
ously for an NRR project [2]; therefore the noding study only
required rerunning the same transient with a coarse-node model.
The nodalization and steady state analysis were completed in FY83,
and the transient calculations were completed this quarter.

The results of this TRAC-PF1 noding study [3] show that the
overall sequence of events and the general trends of the transient
can be predicted quite well with a coarse-node model. The pre-
dicted PCTs for the coarse-node calculation are about 75 K less
than the PCTs predicted by the fine-node calculation. The higher
PCT of the fine-node calculation is attributed to three-dimensional
flow effects in the core. The coarse-node calculation required 13
hours of Cyber-76 CPU time, compared to 61 hours for the fine-node
calculation. On a per-cell basis, the coarse-node model (using 320
mesh cells) ran approximately two times faster than the fine-node
model (using 720 mesh cells).

This quarter also ends the RELAP5/MOD1 independent assessment
project with the completion of the last analyses scheduled (i.e.,
the Semiscale S-UT-8 small break transient analysis), although

1

formal documentation of completed results will extend into the
next quarter.

The S-UT analysis results [4] show that RELAP5/MOD1 calculates
the overall depressurization satisfactorily for a 10% cold leg
break with (S-UT-2) and without (S-UT-1) UHI, until the initiation
of cold leg accumulator flow. The overall loop and vessel mass
distributions were not calculated accurately, resulting in late
time core heatups that were not measured. Oscillations in the
intact loop accumulator flow were both measured and calculated;
however, the calculated period was less than measured and the
source of the oscillations was not the same as that for the test.

For a 5% cold leg break, the predicted depressurization trend
with (S-UT-7) and without (S-UT-6) UHI was different from measure-
ment. The S-UT-6 calculation depressurized to the onset of cold
leg accumulator flow at about the correct time; however, the rate
was not always calculated correctly. The S-UT-7 depressurization
was dominated by surges in the UHI accumulator flow, resulting
from voiding and rapid refilling of the upper head. Calculation of
an excessive condensation rate could also contribute to the surges
in UHI accumulator flow. Similar to the results for the 10% break,
the loop and vessel mass distribution for the 5% break without UHI
were not calculated accurately, resulting in a more severe late
time core heatup than was measured.

The effect of decreasing the core bypass flow from ~2.7% to
~1.5% of the total loop flow for a 5% cold leg break was studied
in test S-UT-8. The measured depression of the core liquid level
to the core inlet elevation at about 200 s in the transient (due
to liquid stacking up in the primary side of the intact loop steam
generator tubes) did not occur in the calculation.

1.0 INTRODUCTION

The TRAC-PF1/MOD1 independent assessment program at Sandia National Laboratories (SNLA) is part of a multi-faceted effort sponsored by the Nuclear Regulatory Commission (NRC) to determine the ability of various systems codes to predict the detailed thermal/hydraulic response of LWRs during accident and off-normal conditions. This program is a successor to the RELAP5/MOD1 independent assessment project performed at Sandia during FY82 and FY83.

The TRAC-PF1/MOD1 code [1] will be assessed against data from various integral and separate effects experimental test facilities. The assessment matrix was formalized during this quarter, and is shown in Table 1.1. The calculated results will also be compared with results from our previous RELAP5/MOD1 independent assessment analyses whenever possible. A few of the tests in our TRAC-PF1/MOD1 matrix (i.e., the LOFT L2-5 and LOBI Al-04R large break tests, the PKL ID1 natural circulation test series and the B&W OTSG separate effects tests) were also in our RELAP5/MOD1 assessment matrix, and will allow such cross-comparison.

The first quarter of FY84 marks the beginning of the TRAC-PF1/MOD1 independent assessment project at SNLA. The code was obtained from Los Alamos National Laboratory in October 1984, and brought up on both our CDC Cyber-76 and Cray-1S computers, as discussed in Section 2.1. TRAC nodalizations for the PKL and B&W OTSG facilities have been developed and calculations begun (described in Sections 2.2 and 2.3, respectively). These tests were chosen as the starting point because we had reasonably complete facility and test documentation from our RELAP5 assessment project, and we needed some PF1/MOD1 experience with relatively simpler tests before beginning full integral system analyses (such as for LOFT and Semiscale).

At the request of the NRC contract monitor, the FY83 and FY84 assessment programs at SNLA were expanded to include a TRAC-PF1 (not PF1/MOD1) noding study for a design-basis 200% cold leg break accident for the Sequoyah UHI plant. This scenario had previously been analyzed for NRR [2] using a detailed fine-node input model; the noding study involved developing a corresponding coarse-node model, and comparing both the results calculated and the execution time required. The nodalization [5] and steady state analysis [6] were completed in FY83; the transient calculations were completed this quarter, with results discussed in Section 3.

This quarter also ends the RELAP5/MOD1 independent assessment project with completion of the scheduled analyses, although formal documentation of completed results will extend into the next quarter. The only calculation actually performed in this quarter was the Semiscale S-UT-8 small break transient analysis, described in Section 4.

Table 1.1   TRAC-PF1/MOD1 FY84 Assessment Matrix

Test	Scenario
LOFT LP-FW-1	Loss-of-Feedwater
LOFT LP-SB-1	Small Break
LOFT L2-5	Large Break
Semiscale S-IB-3	Intermediate Break (21.7%)
Semiscale S-SF-3,5	1 Steam Line, 1 Feed Line Break
Semiscale S-SG-?	2 Steam Generator Tube Ruptures
Semiscale S-PL-3	Loss-of-Power
PKL ID1 Series	Natural Circulation
LOBI A1-04R	Large Break
LOBI BR-1M	Intermediate Break (25%)
Flecht Seaset 31504	Reflood
Flecht Seaset 31701	Reflood
B&W OTSG 28/29	Loss-of-Feedwater
Flecht Seaset 8	Natural Circulation
Neptunus Y05	Pressurizer Behavior
Da 'tmouth	3-Tube CCFL
Bankoff	Condensation
Bankoff	Multi-Tube CCFL

2.0 TRAC-PF1/MOD1 ASSESSMENT

The TRAC-PF1/MOD1 assessment matrix for FY84 was finalized this quarter. Discussions were held with the NRC contract monitor near the end of October to decide which LOFT tests we were to analyze with TRAC-PF1/MOD1. We also suggested a number of new separate effects and integral effects tests for possible replacement of the originally scheduled RELAP5/MOD2 assessment tasks. The basic matrix is as presented at the Denver Assessment Meeting (November 15-16, 1983). The Semiscale S-SF series tests have been chosen to be S-SF-3 and S-SF-5. (The S-SG tests remain to be determined since the test series is not yet complete.)

Several members of the Sandia staff attended the TRAC-PF1/MOD1 Workshop at LANL on December 6-7, 1983.

2.1 Code Status

Early in the quarter, version 11.0 of TRAC-PF1/MOD1 was installed on the CDC Cyber-76 at Sandia, which uses the SCOPE 2.1 operating system. It was also installed on our Cray-1S, which uses the COS operating system. Installation on both mainframe machines will allow us more flexibility in performing our assessment analyses if the work load on a given machine is particularly heavy for an extended period of time.

Part of the installation procedure involved making local modifications to the code incorporating the Sandia quality assurance algorithms in TRAC-PF1/MOD1. These algorithms, which are similar to the ones we used for our RELAP5 assessment program, automatically provide the user with all the information needed to identify the code modifications used for any particular run. There is no need for the user to manually change any Hollerith text fields in the code and the system can only be defeated by non-standard use of the load instructions for the code.

The four sample problems transmitted on the tape containing the MOD1 code were run on the Cyber-76 and on the Cray-1S versions of the code. As a result, we discovered an error in memory allocation which affected some problems running on the Cray version; the error was fixed by LANL after we identified the "bug" for them. A UPI plant large break LOCA deck (developed for an NRR project) which we had run on an earlier version of PF1 was also used to test the Cray version of MOD1. However, even after our own overlay revisions to MOD1 to increase the size of the main data storage array to 26900, the UPI problem still would not fit on the Cyber-76 and thus could not be used as a test problem for

5

that system. This result indicates that most of our integral-test assessment calculations will probably have to be run with the Cray version of TRAC unless further overlaying of the code is done.

Updates to create TRAC-PF1/MOD1 Version 11.1 were received from LANL during the quarter via their new VAX node, which allows exterior-to-LANL user access to selected code updates and other TRAC-related information. Those updates were incorporated into our code on both machines. (The memory allocation correction mentioned above was part of those updates.) Since most of the updates to create Version 11.1 were correcting actual code errors, we plan to use that version for our initial assessment calculations.

The Sandia-generated plot routines we previously used with TRAC-PF1 were adapted to work with the TRAC-PF1/MOD1 graphics file during the quarter. The capability to plot experimental data was added to the TRAC plot routines, as well as several other modifications to make the TRAC plot package more compatible with our RELAP5 plot routines.

Two other modifications were made to the plot programs for both TRAC and RELAP5 during the quarter. The first change allows various quantities on the plot tapes to be displayed as a function of distance along the piping network. Previously, special modifications were required for each individual case of interest. The second change made to the two plot packages allows any of the standard plot variables to be output from the plot routines in the experimental data format; this new feature was added to simplify cross-plotting of results between Cray and Cyber-76 runs and between RELAP5 and TRAC runs.

2.2 PKL Natural Circulation Tests

The Primarkreislaufe (PKL) test facility [7], located at Erlangen, West Germany, is a 1/134-scale three-loop model of a four-loop PWR. All elevations correspond to a full-scale system, so that gravitational terms are correctly simulated. Core power is provided by 340 electrically heated rods. The facility is shown in Figure 2.2.1.

The ID1 series of tests [8] was designed to study the natural circulation modes occurring during small break situations in which the primary system was slowly losing inventory. In a continuous operational mode, data for twelve different inventories was recorded, with the test notations of ID1-4 to ID1-15. These data points covered the entire range of potential system response from subcooled natural circulation to reflux cooling, as shown in Table 2.2.1.

This test series had previously been analyzed during our RELAP5/MOD1 independent assessment project [9]. In those analyses, we had explicitly modelled all three loops in the primary system. Closer inspection of the data and calculated results showe? no significant loop asymmetries (although some long-period loop-to-loop oscillations were calculated during reflux cooling). A single-lumped-loop RELAP5 model was recently developed, and the results showed similar good agreement with data for ID1-4 as obtained with the original three-loop model. We therefore felt reasonably confident that a single-lumped-loop model could be used for our TRAC analyses (saving some computer time).

The TRAC nodalization developed is shown in Figure 2.2.2; it consists of 20 components with a total of 89 cells. The vessel is modelled using the 1-D CORE component. Because the pressurizer is valved out of the system during most of the tests, we did not model it explicitly, but simply applied a pressure boundary condition to one of the free junctions in the model (at the top of the vessel external downcomer). The annular deadspace corresponding to the interior vessel downcomer (not used in these tests) is modelled, as is the system metal mass. However, several inherent limitations of TRAC heat slabs prevented us from modelling all the heat loss paths explicitly.

This TRAC-PF1/MOD1 input deck was then used to simulate the ID1-4 single-phase natural circulation test. We found that the single-phase natural circulation rate predicted by this first run (5.35 kg/s) was substantially higher than measured (4.55 kg/s); increasing the code hardwired wall roughness by a factor of eight to a value more representative of that published by PKL only reduced the TRAC predicted flow rate to 5.22 kg/s. This result suggested that we needed to develop a much better understanding of how to geometrically model a facility with respect to piping area changes and wall friction losses with the TRAC code. (There are substantial differences between RELAP5 and TRAC in this regard and RELAP5 had done exceptionally well in the prediction of single-phase natural circulation rates.)

Because of our limited TRAC-PF1 and TRAC-PF1/MOD1 experience and the fact that there are no published TRAC user guidelines in this area, we have resorted to studying the detailed models for area changes used by each of the two codes, and we are trying to come up with consistent modelling techniques. It currently appears that simple guidelines for determining input areas and hydraulic diameters can be used to produce the same or similar single-phase form losses in some circumstances, but not in others. This study of the detailed area-change models will be completed next quarter, the input deck revised, and these PKL analyses will be continued.

Table 2.2.1 PKL ID1 Test Results

ID1	Bundle Power	Water** Inventory	Mode of Energy Transport	Flow Rate Ṁ	Δθ$_{P-S}$	P$_P$	P$_S$	ΔP$_{P-S}$
-	kW	%		KG/S	K	BAR	BAR	BAR
4	402	100	Subcooled Natural Circulation	4.5	17	28.8	18.8	10.0
5	625	100	Subcooled Natural Circulation	5.4	25	29.7	17.8	11.9
6*	404	99	Single Phase Natural Circulation	5.4	16	30.1	23.3	6.8
7*	405	96	Single Phase Natural Circulation	4.9	16	30.0	23.3	6.7
8	409	95	Two Phase Circulation	9.1	3-5	30.0	28.8	1.2
9	410	93	Two Phase Circulation	7.5	3-5	29.8	28.7	1.1
10	413	87	Two Phase Circulation	4.2	3-5	30.5	29.6	0.9
11	411	80	Two Phase Circulation	3.2	3-5	30.0	29.1	0.9
12	412	84	Two Phase Circulation	1.7	3-5	30.2	29.7	0.5
13	412	80	Reflux Condenser	0	2-4	30.2	30.0	0.2
14	411	51	Reflux Condenser	0	2-4	29.5	29.5	0
15	641	53	Reflux Condenser	0	2-4	29.9	29.1	0.1

*Some Steam in Upper Plenum
**Primary Side Water Inventory (Pressurizer Not Included)

8

2.3 B&W OTSG LOFW TESTS

A steady state (run 28) test and its associated loss-of-feedwater (LOFW) transient (run 29) in the Babcock & Wilcox (B&W) 19-tube once-through steam generator (OTSG) test facility [10] is currently being analyzed as part of the TRAC-PF1/MOD1 independent assessment program at Sandia National Laboratories. This test has also been analyzed as part of our RELAP5/MOD1 independent assessment project. [11]

The primary objectives of the B&W steam generator tests were to determine steady state operating conditions such as mass inventory, temperatures, and pressure drops, and to determine the secondary steam flow during a LOFW transient.

The test steam generator is a single pass, counterflow, tube and shell heat exchanger. The secondary side feedwater enters the top of the downcomer and mixes with steam bled from the boiler through an aspirator line. This steam heats the feedwater to saturation before entering the boiler region of the secondary. The primary and secondary side flows were scaled directly by the number of tubes in a full-scale steam generator (19:15,500).

The noding diagram for the TRAC OTSG model we developed is shown in Figure 2.3.1. There are 28 mesh cells on the primary side and 43 cells on the secondary side. The lower portion of the boiler region was finely noded in order to better resolve the axial fluid distribution. The geometric information and the noding strategy for this TRAC nodalization were taken from our RELAP5 model [11]. The number and location of the mesh cells in both models therefore match exactly.

One difficultly that arose when converting the RELAP5 model to a TRAC model involves the hydraulic diameters. RELAP5 uses cell-centered values for hydraulic diameter whereas TRAC uses cell-edged values. Therefore, a one-to-one conversion was not possible. Several of the cell edges occur at tube support plates (indicated by x's on Figure 2.3.1), which represent a substantial reduction in flow area. We are currently attempting to develop some guidelines on how to correctly model the associated wall friction and form losses, possibly through adjustment of the hydraulic diameter and flow areas, and through addition of user-input form-loss coefficients at these cell edges. In our first calculations, the hydraulic diameter at the tube support plates was simply set equal to the hydraulic diameter of the tube bundle and no additional form losses were included.

We input the heated equivalent diameter used for heat transfer as the minimum tube-to-tube spacing, as was done in the RELAP5 model. Previous experience with both RELAP5 and TRAC have indicated that this is a more representative value for flow through a bank of tubes than using the hydraulic diameter of the adjacent cell.

The results of a preliminary steady state calculation give measured and calculated primary side parameters that are in excellent agreement, as are the steam exit temperatures. However, the predicted boiler ΔP is about 15% too low and the predicted secondary mass is too high.
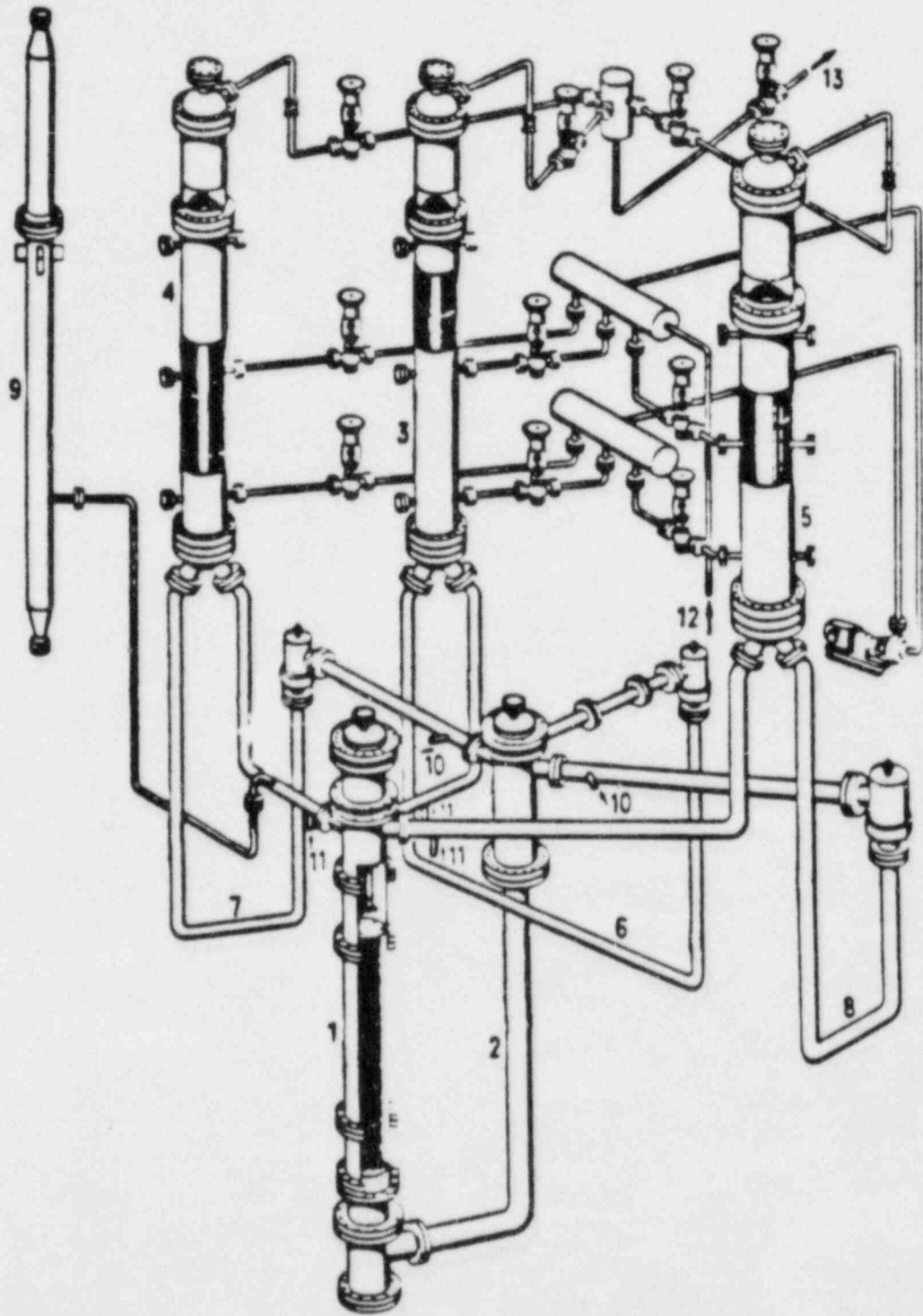
1   Rod Cluster Container   8   Pump Bend 3
2   Downcomer   9   Pressurizer
3   Steam Generator 1 (broken loop) 10 Cold Injection Point
4   Steam Generator 2 (single loop) 11 Hot Injection Point
5   Steam Generator 3 (double loop) 12 Coolant Supply
6   Pump Bend 1   13 Steam Relief Point
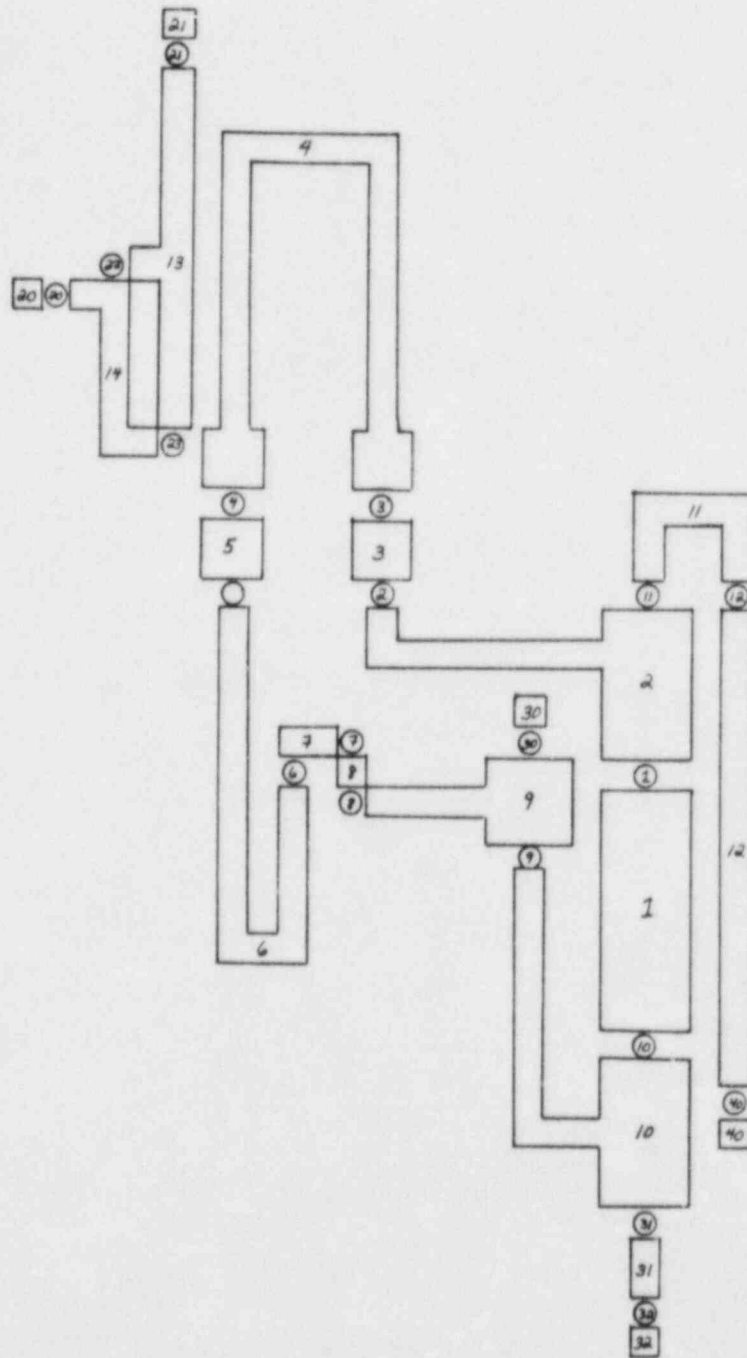7   Pump Bend 2

Figure 2.2.1   PKL Test Configuration

Figure 2.2.2 TRAC-PF1/MOD1 Nodalization for PKL
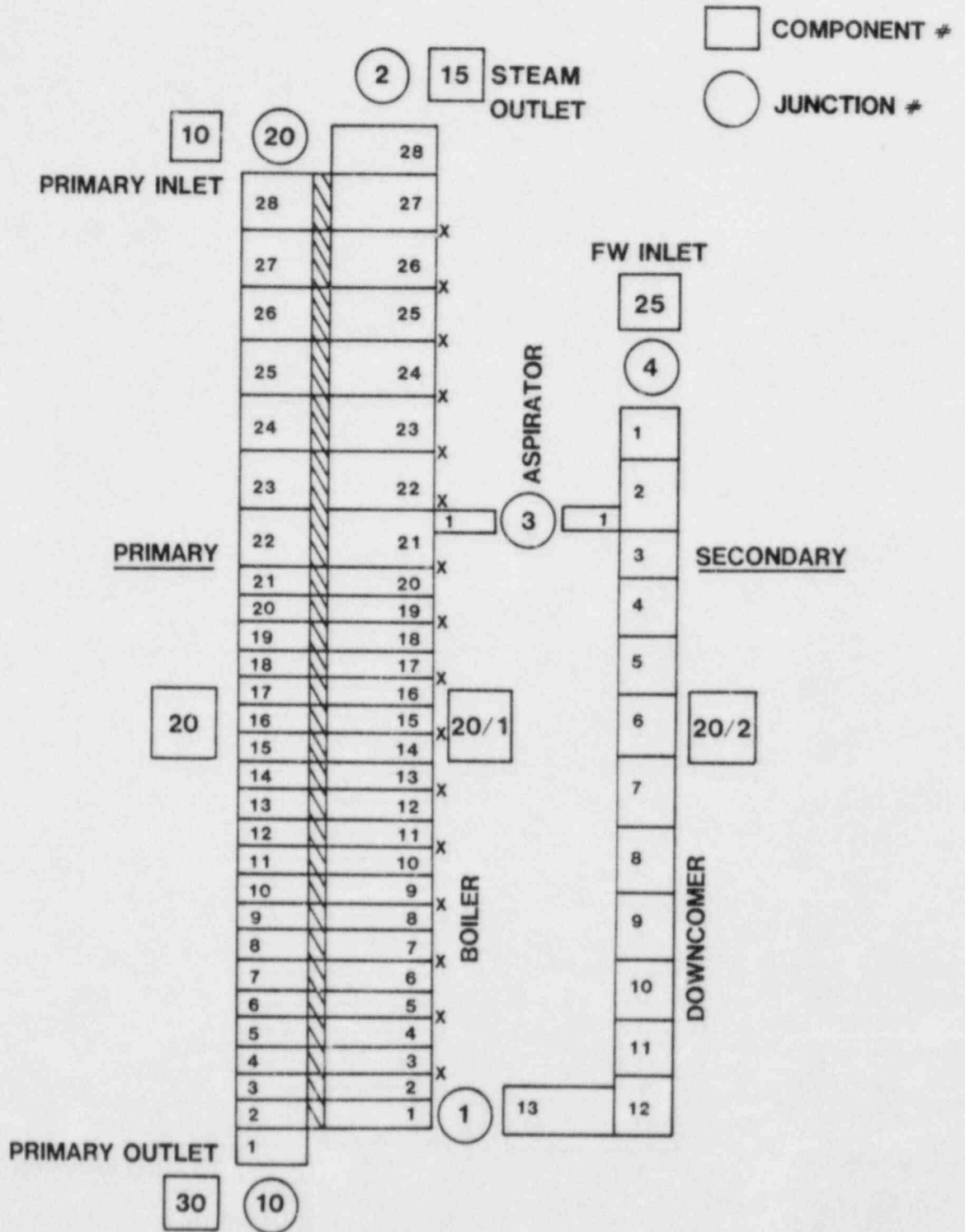Test Facility

12

Figure 2.3.1   B&W Once-Through Steam Generator
TRAC Noding Diagram

3.0 TRAC-PF1 NODING STUDY

Several years ago, a project was funded at Sandia by the Office of Nuclear Reactor Regulation (NRR) to investigate a large-break LOCA for a Westinghouse PWR equipped with upper head injection (UHI). Several computer codes were used for this investigation, including RELAP4/MOD5, FRAP-T4, FLOOD and TOODEE2; the use of all these codes in sequence was required to simulate the complete transient including blowdown, refill and reflood. Later, the same accident scenario was analyzed at Sandia using a single code, TRAC-PD2, and then, because of difficulties encountered with PD2, TRAC-PF1 (version 7.2) was used. [2] The final TRAC-PF1 calculation was run to 105 s using a "fine-node" input model. Recently, it was decided by the Office of Nuclear Reactor Research (RES) that this already-completed calculation offered an opportunity for TRAC noding studies, and a TRAC-PF1 "coarse-node" calculation has therefore been performed as part of our assessment effort.

Both the fine-node and coarse-node models represent a four-loop Westinghouse PWR equipped with UHI accumulators in addition to cold leg accumulators. Descriptions of both input models, the corresponding TRAC noding diagrams, and results of steady state calculations have been given in previous quarterly reports. [5,6] However, some additional comments concerning the input models are given here, before presenting the transient results.

The fine-node core contained a different radial power profile than the coarse-node core, because of the different number of radial regions. Therefore, supplemental fuel rods were included in the coarse-node model with peaking factors chosen to match the linear heat generation rates of the fine-node rods. These supplemental rods do not feed back to the thermal/hydraulics, but allow convenient comparison of rod temperatures.

Of special interest in the models are the different methods of modelling the guide tubes (GTs) and support columns (SCs). The GTs and SCs in the fine-node vessel were modelled by defining stacks of r-θ cells in the upper plenum to have zero radial and azimuthal flow areas. The GTs and SCs in the coarse-node vessel were modelled by connecting one-dimensional (1-D) pipe components from the core to the upper head. Pipes were used in the coarse-node model because of an insufficient number of r-θ stacks. One-dimensional pipes had not been used in the fine-node calculation because only a drift-flux model was available for pipes in TRAC-PD2. Although TRAC-PF1 uses a two-fluid treatment in the 1-D pipes, the original input model was not changed when code versions were changed.

15

Also worth noting is the asymmetric azimuthal noding in the coarse-node vessel. Unequal sectors were chosen such that the volume ratios of the loop-to-azimuthal vessel sector were equal, i.e., the combined loop (representing the three intact loops) was connected to an azimuthal sector proportionately larger than the sector connected to the single broken loop.

The results using the coarse-node model were very similar to those from the fine-node calculation for all phases of the LOCA. Figures 3.1 and 3.2 compare the mass flows for the pump-side and vessel-side breaks, respectively; as can be seen, the agreement is extremely good. The difference in integrated pump-side break mass flow over the entire LOCA is less than 0.5%. However, the coarse-node integrated vessel-side break mass flow is about 9.0% lower than in the fine-node calculation. This deviation occurs mainly during reflood when the fine-node calculation predicts large manometer oscillations between the core and downcomer, with large slugs of liquid swept out of the break as a result. Although the same oscillations are seen in the coarse-node calculation, their amplitude is much smaller, possibly due to the reduced (by ~30%) rate of cold leg accumulator injection in the coarse-node calculation. Because less liquid entered the vessel, the downcomer elevation head (which drives these manometer oscillations) is much smaller. The downcomer liquid volume fraction for both cases is shown in Figure 3.3, where the oscillations can easily be seen.

A possible cause of the lower cold leg accumulator flow in the coarse-node analysis is the combining of three intact loops into one loop. In the fine-node calculation, liquid penetration into the downcomer from the cold legs was intermittent. Flow stopped, or slowed considerably, when vapor from the downcomer was drawn into the cold leg (due to condensation) and prevented the liquid from entering the vessel. When the leading surface of the incoming liquid was heated by the hot vapor, condensation decreased and penetration resumed. At least one of the three cold legs was delivering liquid to the downcomer at any given time.

In contrast, the coarse-node model contains only one equivalent intact cold leg. Therefore, condensation of vapor by accumulator liquid occurred only in that cold leg, reducing the injection of liquid into the vessel. The vessel liquid mass for both cases is shown in Figure 3.4. Between 40 and 70 s, much of the cold leg accumulator liquid was collecting in the cold leg in the coarse-node calculation. At 70 s, the rate of condensation slowed sufficiently to allow liquid to flow into the vessel. It is interesting that, although the coarse-node calculation underpredicted the amount of bypass by 20,000 kg, it also underpredicted the amount of cold leg accumulator injection by 25,000 kg, compared to the results in the fine-node calculation.

16

Therefore, about the same amount of liquid entered the vessel for both cases, and, by 100 s, the vessel inventory for both cases was approximately equal. The lower plenum liquid volume fraction, shown in Figure 3.5, also shows the sudden penetration of liquid at 70 s. The HPI, LPI, and upper head accumulator flows were nearly identical for both cases.

The vapor fraction in the top of the upper head is shown in Figure 3.6. The upper head initially was emptying at the same rate in both calculations. However, during the closing of the upper head accumulator surge line valve (20-25 s), liquid was drawn back up the SCs and GTs into the upper head in the fine-node calculation. Figure 3.7 shows the pressure in the upper head for both cases. The drop in pressure in the fine-node calculation during the valve closing, which seems to be related to the clos- ing of the valve, was the reason for the flow into the upper head from the core. The valve model and accumulator surge line piping were identical for both cases, with the only difference in the models being the volume of the upper head cells to which the lines connect and the way in which the GTs and SCs were modelled. The fine-node upper head response to the valve closure is not totally understood; however, the coarse-node response seems more reasonable. Overall, the effect this pressure drop has on the fine-node transient seems to be minimal when compared to the coarse-node transient.

The sequence of events for both calculations are compared in Table 3.1. As can be seen, the agreement in the timing sequence is extremely good.

Table 3.1 Sequence of Events

| | Time (s) | |
Event	Fine-Node	Coarse-Node
Reactor trip	0.0	0.0
UHI accumulator on	.512	.557
Initial PCT	2.63	2.50
Upper head begins to flash	4.0	4.0
Cold leg accumulator on	17.0	17.2
UHI shutoff valve closes	20.4-25.0	20.7-25.7
Cold leg ECCS bypass period	17-33	17-35
Beginning of core recovery	72	70
Second PCT	81	80

Figures 3.8 through 3.12 compare the clad temperatures for both cases at various axial locations. (The axial elevations are referenced to the bottom of the reactor vessel; the bottom of the core is at 3.087 m, the core midplane is at 4.917 m and the top of the core is at 6.747 m.) These temperatures are for rods located in the first or inner radial region of the core for both cases. (The first two radial regions of the fine-node core model were combined to form the inner radial region of the coarse-node model.) Although the volumes of the hydrodynamic cells in which the rods are located are different (due to the different vessel noding), these rods have the same linear power generation rate, 6.28 kW/ft. This was possible because of the supplemental rods included in the coarse-node model. Figures 3.13 through 3.17 show the clad temperatures for rods with a linear power generation rate of 5.70 kW/ft. The coarse-node calculation, on average, slightly underpredicts the clad temperature compared to the fine-node calculation; however, this is not true for all locations in the core at all times.

Another way to compare the clad temperatures is by looking at the average-powered rods from both models. An average-powered rod from each of the first two radial regions of the fine-node model can be compared to the average-powered rod in the first radial region of the coarse-node model. The first radial region and second radial region fine-node rods have linear power generation rates of 6.28 kW/ft and 5.70 kW/ft, respectively, while the coarse-node first radial region rod has a rate of 5.99 kW/ft (i.e., the volume-weighted average of the two fine-node rods). Therefore, one would expect the clad temperature of the coarse-node rod to fall somewhere between the clad temperatures of the two fine-node rods. This was not found to be the case throughout the core, as shown in Figures 3.18 and 3.19. These plots compare fine-node calculation clad temperatures to coarse-node calculation clad temperatures for two different azimuthal sectors of the core, at the core midplane. Figure 3.18 shows clad temperatures for rod 1 of the coarse-node model and rods 2 and 10 of the fine-node model. (These rods are in the azimuthal sector adjacent to the broken loop cold leg.) Figure 3.19 shows clad temperatures for rod 4 of the coarse-node model and rods 8 and 16 of the fine-node model. (These rods are in the azimuthal sector adjacent to an intact loop hot leg.) The coarse-node rod temperature does fall between that of the fine-node rods in Figure 3.18, but not in Figure 3.19.

This behavior is due to the asymmetric vessel geometry, which leads to complex multi-dimensional flow patterns within the core. Only a fine-node model has the noding detail necessary to account for such three-dimensional effects as liquid channeling past rods located directly beneath support columns and guide tubes. A

18

coarse-node model can only predict the average flow through the core. Although the complex flow patterns predicted in the fine-node calculation had an effect on the predicted clad temperatures, the average, or integral, response of the clad temperatures was predicted very well using the coarse-node model.

The peak clad temperatures during blowdown and reflood for both cases are shown in Table 3.2. The predicted PCTs for the coarse-node calculation are about 75 K less than the PCTs predicted for the fine-node calculation.

Table 3.2 Peak Clad Temperatures

PCT(K)

	Fine-node	Coarse-node
Blowdown:	1025	952
Reflood:	990	915

The run-time statistics are shown in Table 3.3. The coarse-node calculation took 13 hours of Cyber-76 CPU time, compared to 61 hours for the fine-node calculation, a reduction factor of approximately five in the total run time. The CPU time divided by the transient time per cell was 2.8 for the fine-node and 1.3 for the coarse-node, for a reduction factor of approximately two. So, on a per-cell basis, the coarse-node calculation ran about two times faster than the fine-node calculation. Of particular interest, however, is the last column. The CPU time per timestep per cell is a measure of the computational efficiency of the code, and is sometimes referred to as the "grind time". Because the fine-node model has a larger percentage of 3-D vessel cells, one would expect a larger grind time for that calculation. However, the coarse-node calculation was found to have a slightly larger grind time. Two possible explanations for this exist. First, more vessel source connections were required in the coarse-node model because of the way the guide tubes and support columns were modelled. And second, each r-θ channel of the fine-node core contained one average rod and one supplemental rod, whereas, each r-θ channel of the coarse-node core contained one average rod and two supplemental rods. This study was really not sufficient to allow a determination of the exact causes of the high values of grind time for the coarse-node calculation. Additional calculations and parametric studies would be required to achieve a better understanding of the code's computational efficiency.

19

The results of this noding study indicate that a reasonable prediction of the transient can be obtained using a coarse-node model with a considerable savings in computer time compared to a fine-node model. The overall sequence of events and general trends of the transient were predicted quite well. However, a fine-node model is required if one wishes to investigate multi-dimensional core flows.

Table 3.3   Run-Time Statistics

Model	CPU (s)	Transient Time (s)	Number of Steps	Average Timestep Size (ms)
Coarse-node:	45360	111.4	15862	7.02
Fine-node	221505	105.0	36939	2.84

Model	CPU/s	CPU/s/cell	CPU/step (s)	CPU/step/cell (ms)
Coarse-node:	407.2	1.273	2.860	8.94
Fine-node	2109.6	2.849*	5.996	8.086*

*Adjusted to account for the different number of cells used during different phases of the calculation.
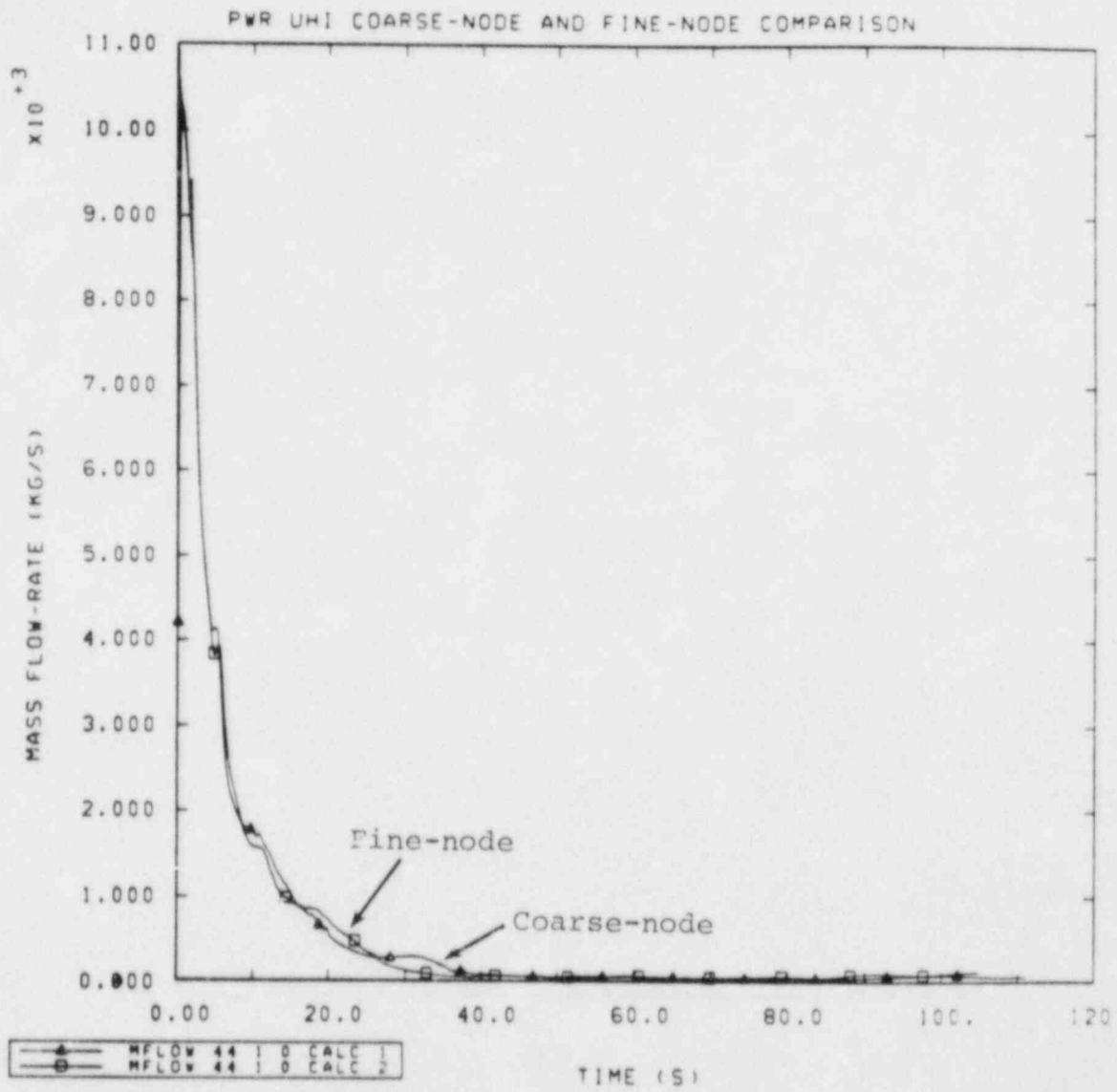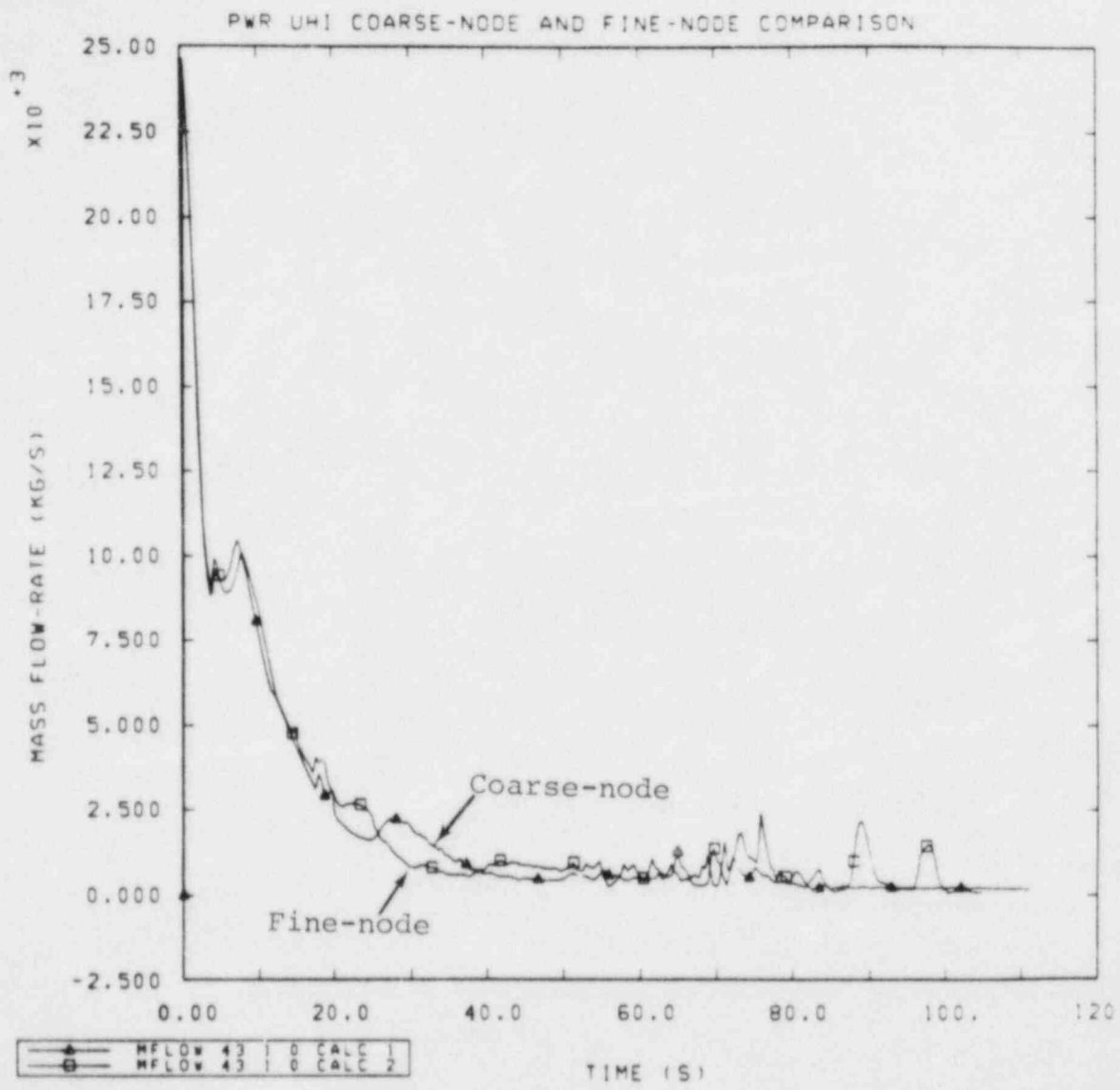
20

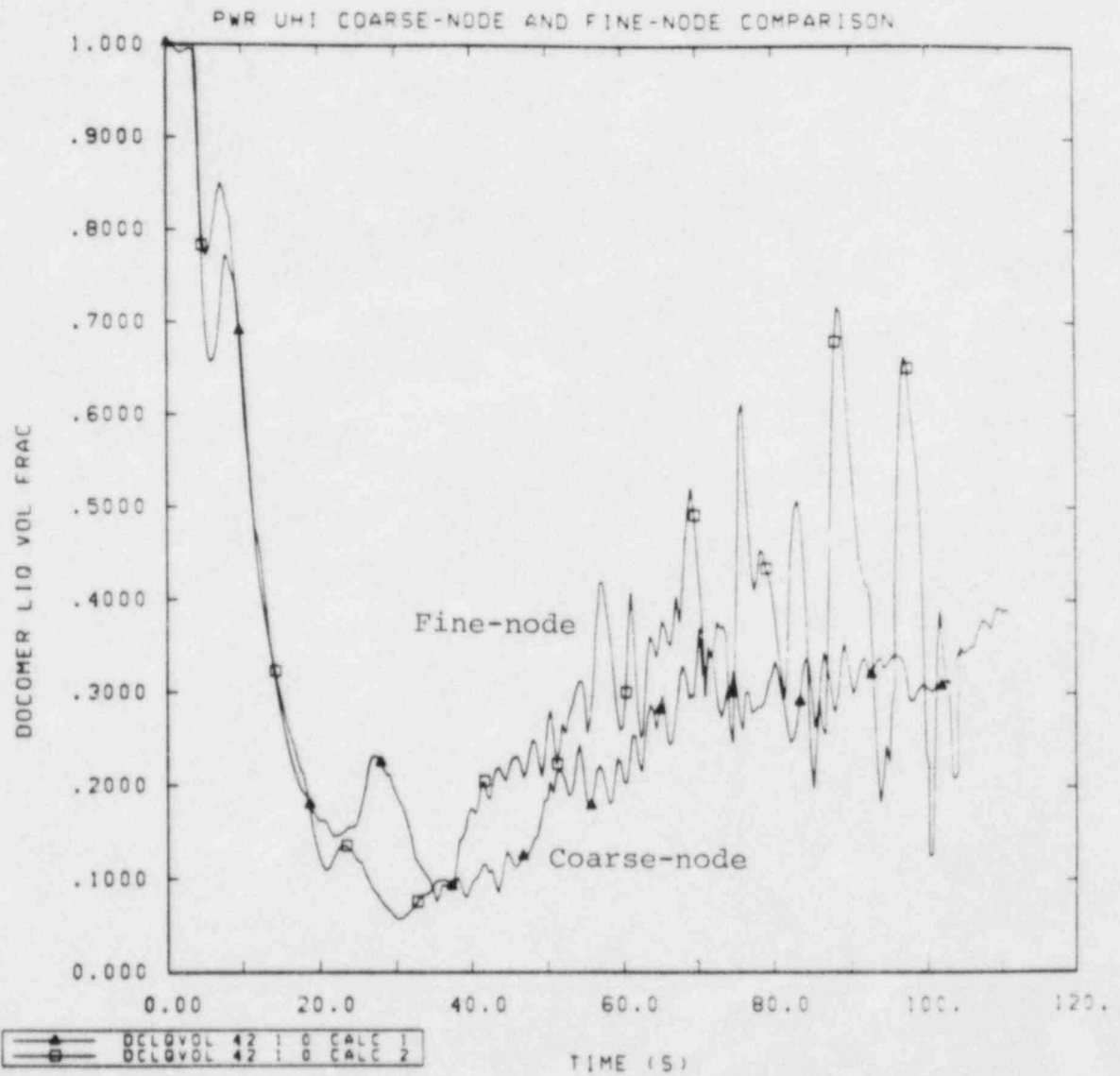Figure 3.1 Pump-side Break Mass Flow

Figure 3.2   Vessel-side Break Mass Flow
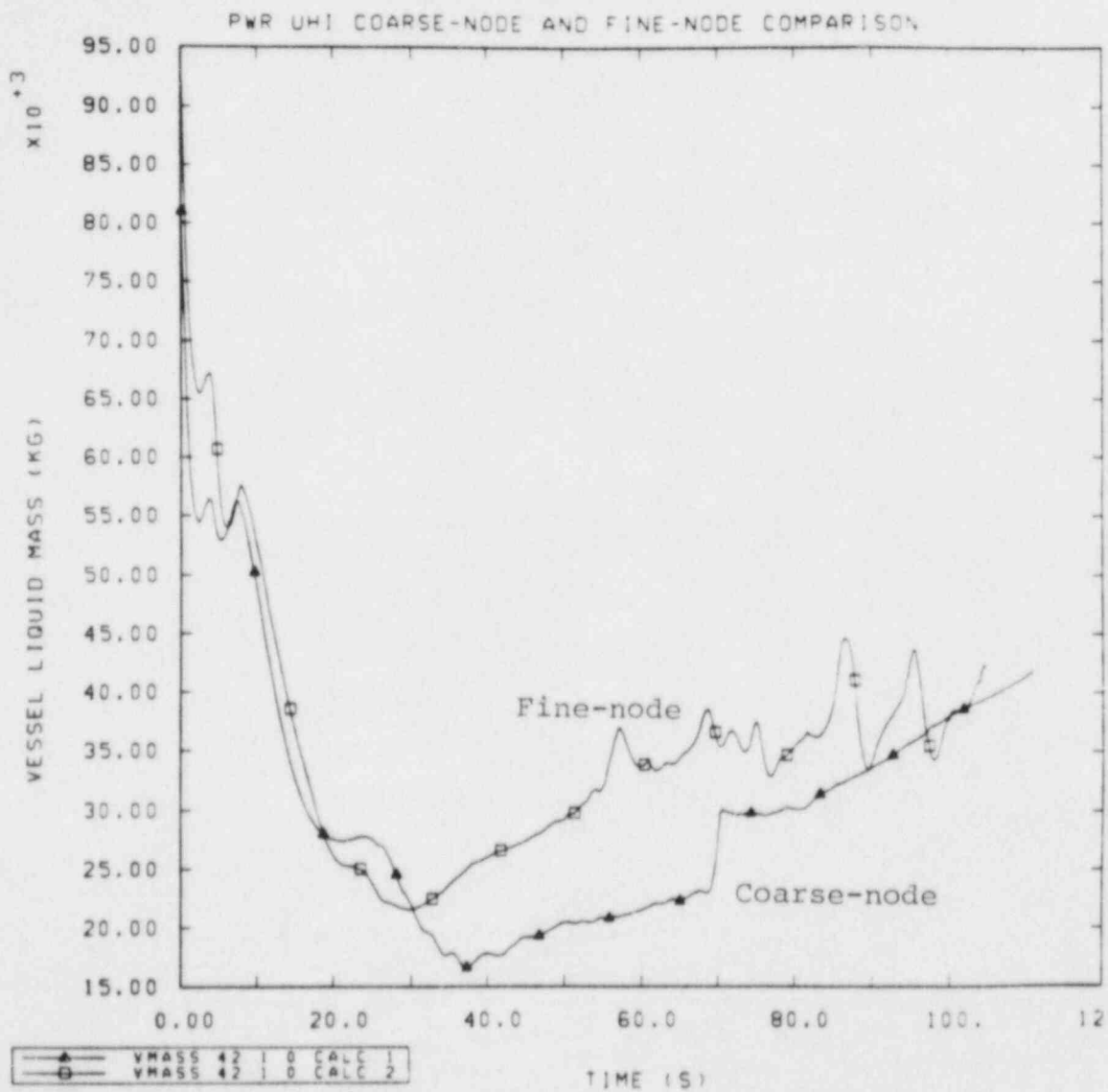
22

Figure 3.3   Downcomer Liquid Volume Fraction

23

Figure 3.4   Vessel Liquid Mass

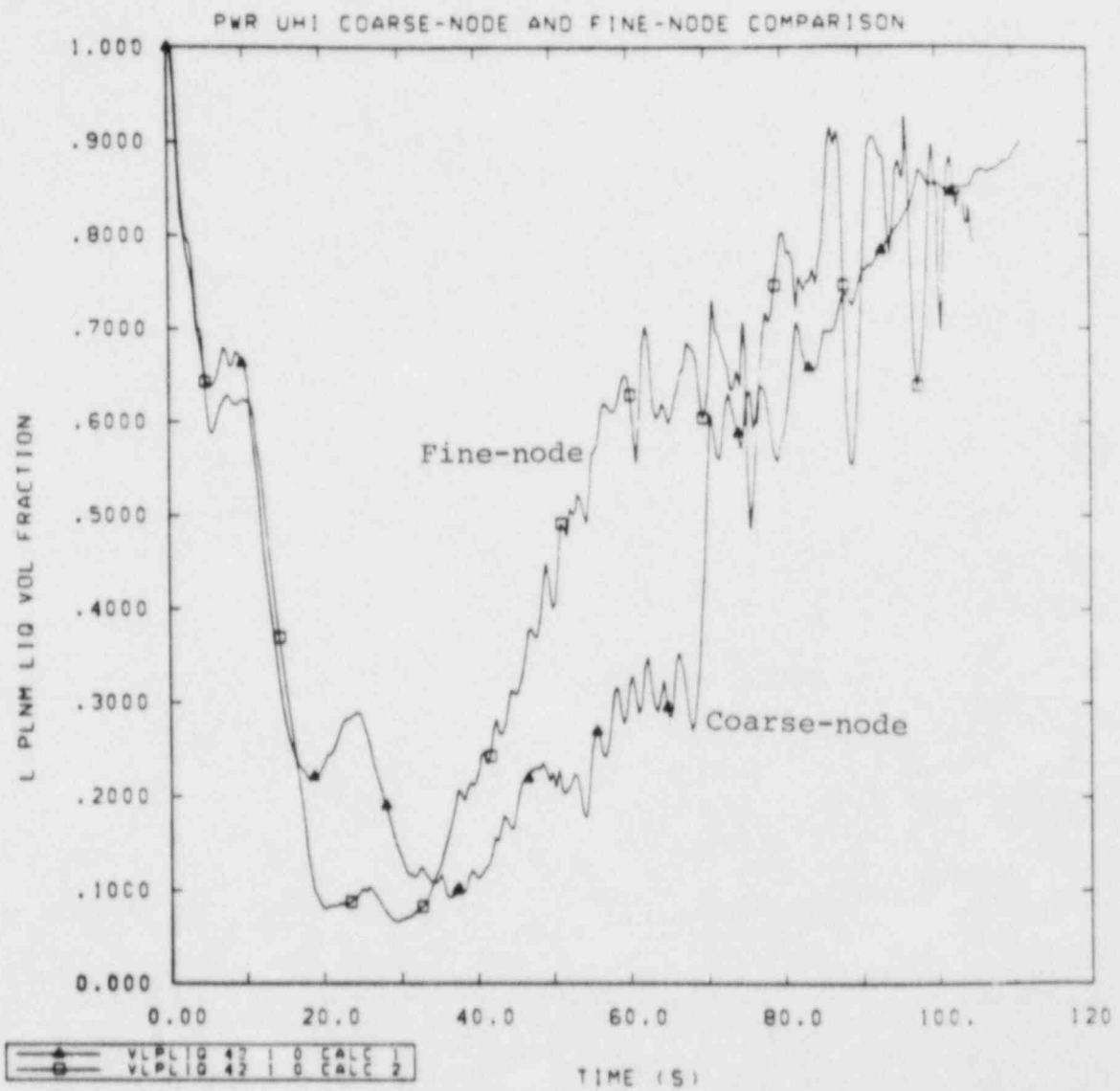24

PWR UHI COARSE-NODE AND FINE-NODE COMPARISON

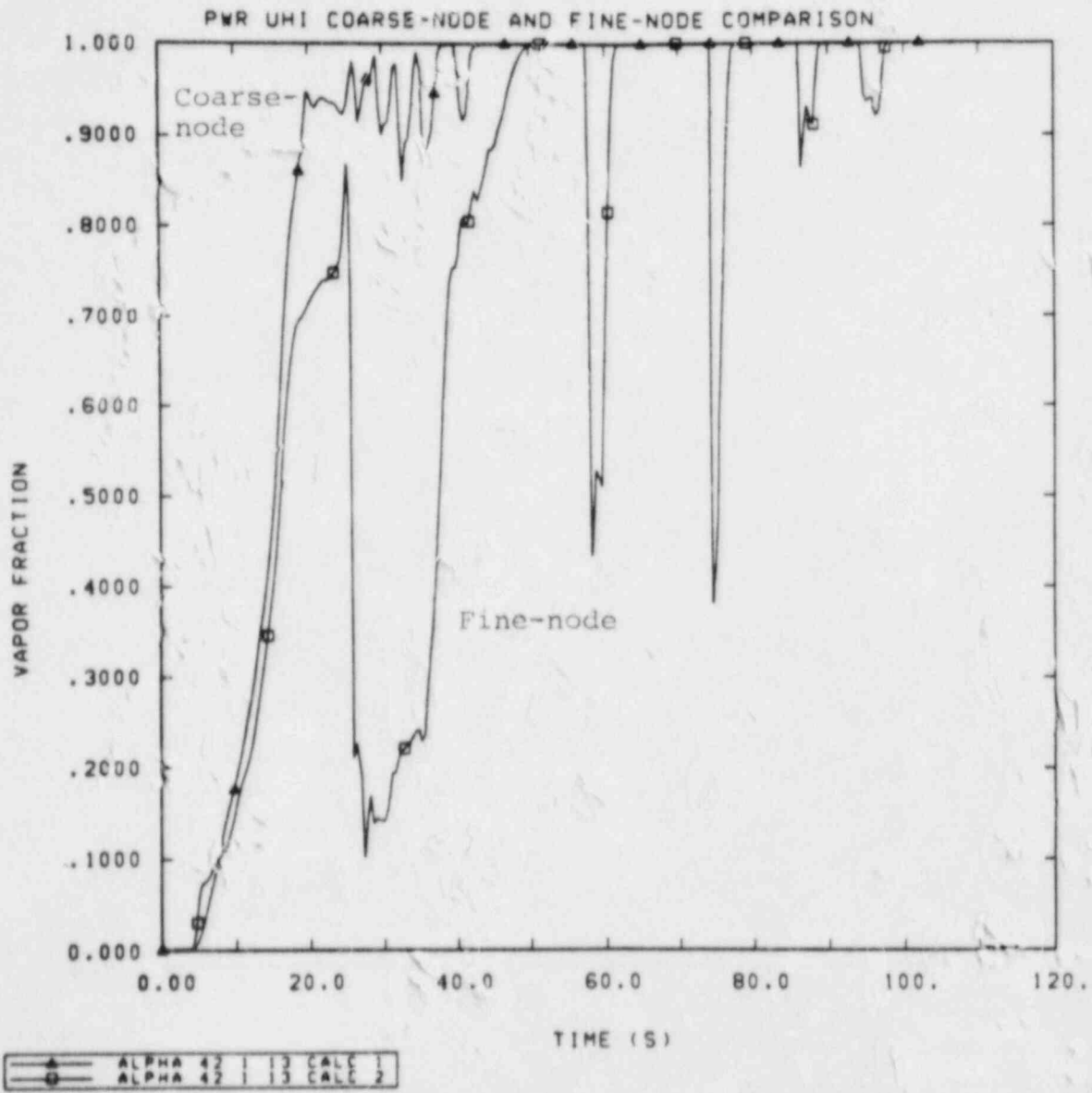Figure 3.5   Lower Plenum Liquid Volume Fraction

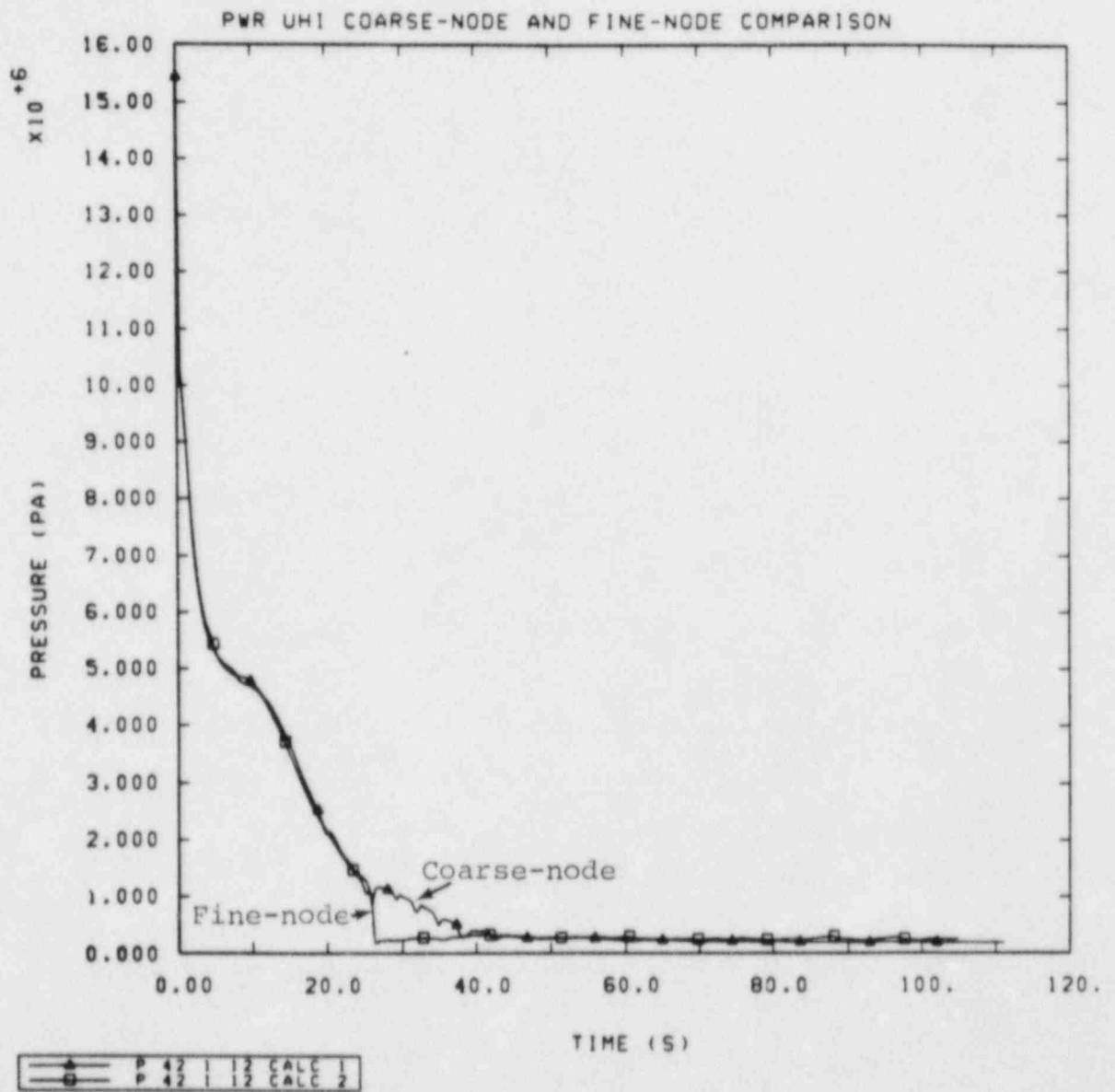Figure 3.6 Upper Head Vapor Fraction

26

Figure 3.7 Upper Head Pressure
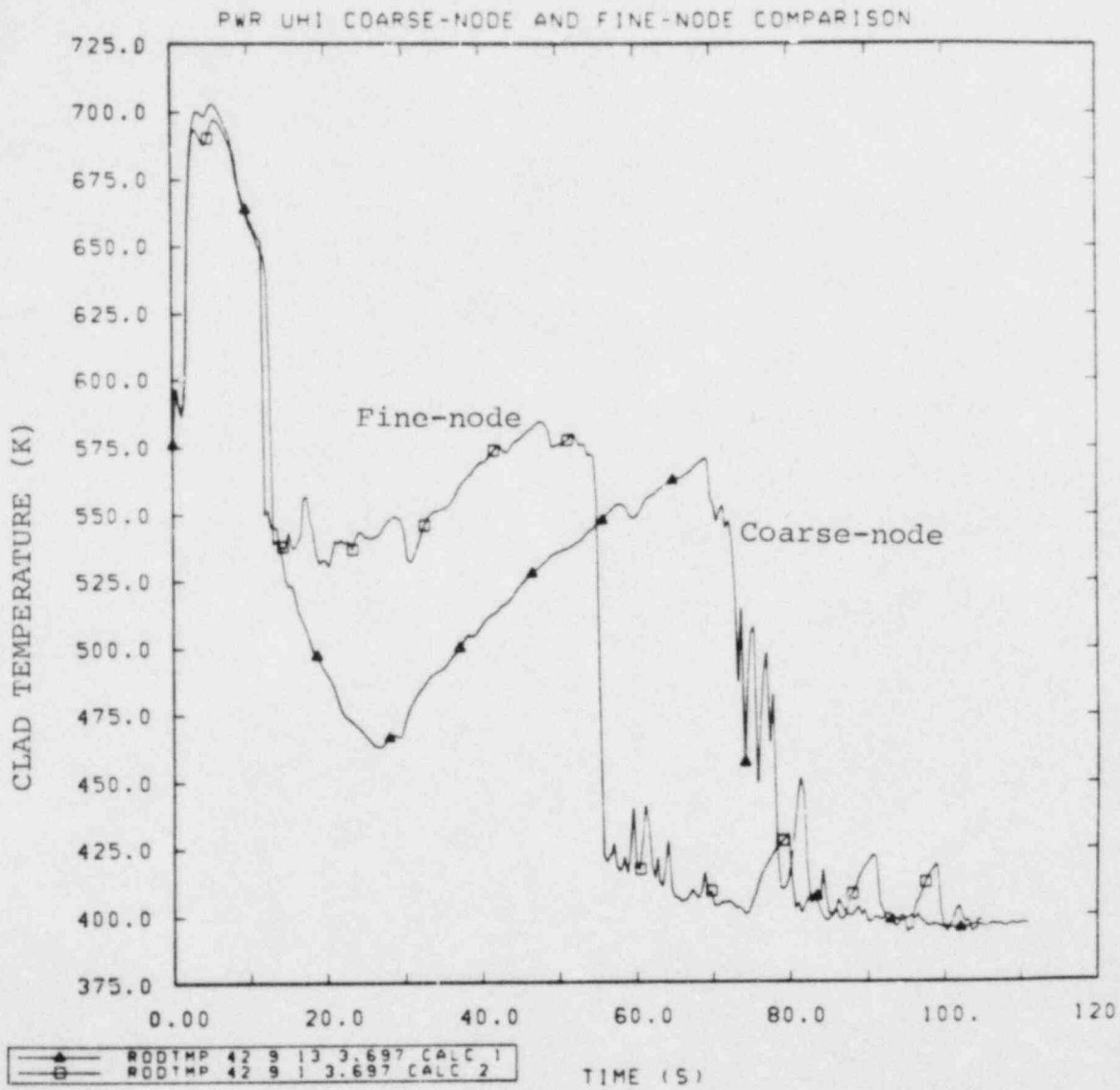
Figure 3.8 Clad Temperature; Axial Elevation: 3.697 m,
Average Linear Power Generation Rate: 6.28 kW/ft

Figure 3.9   Clad Temperature; Axial Elevation: 4.307 m,
             Average Linear Power Generation Rate: 6.28 kW/ft

29

PWR UHI COARSE-NODE AND FINE-NODE COMPARISON

Figure 3.10   Clad Temperature; Axial Elevation: 4.917 m,
Average Linear Power Generation Rate: 6.28 kW/ft

30

Figure 3.11 Clad Temperature; Axial Elevation: 5.527 m, Average Linear Power Generation Rate: 6.28 kW/ft

31

Figure 3.12 Clad Temperature; Axial Elevation: 6.747 m,
Average Linear Power Generation Rate: 6.28 kW/ft

32

Figure 3.13 Clad Temperature; Axial Elevation: 3.697 m,
            Average Linear Power Generation Rate: 5.70 kW/ft

33

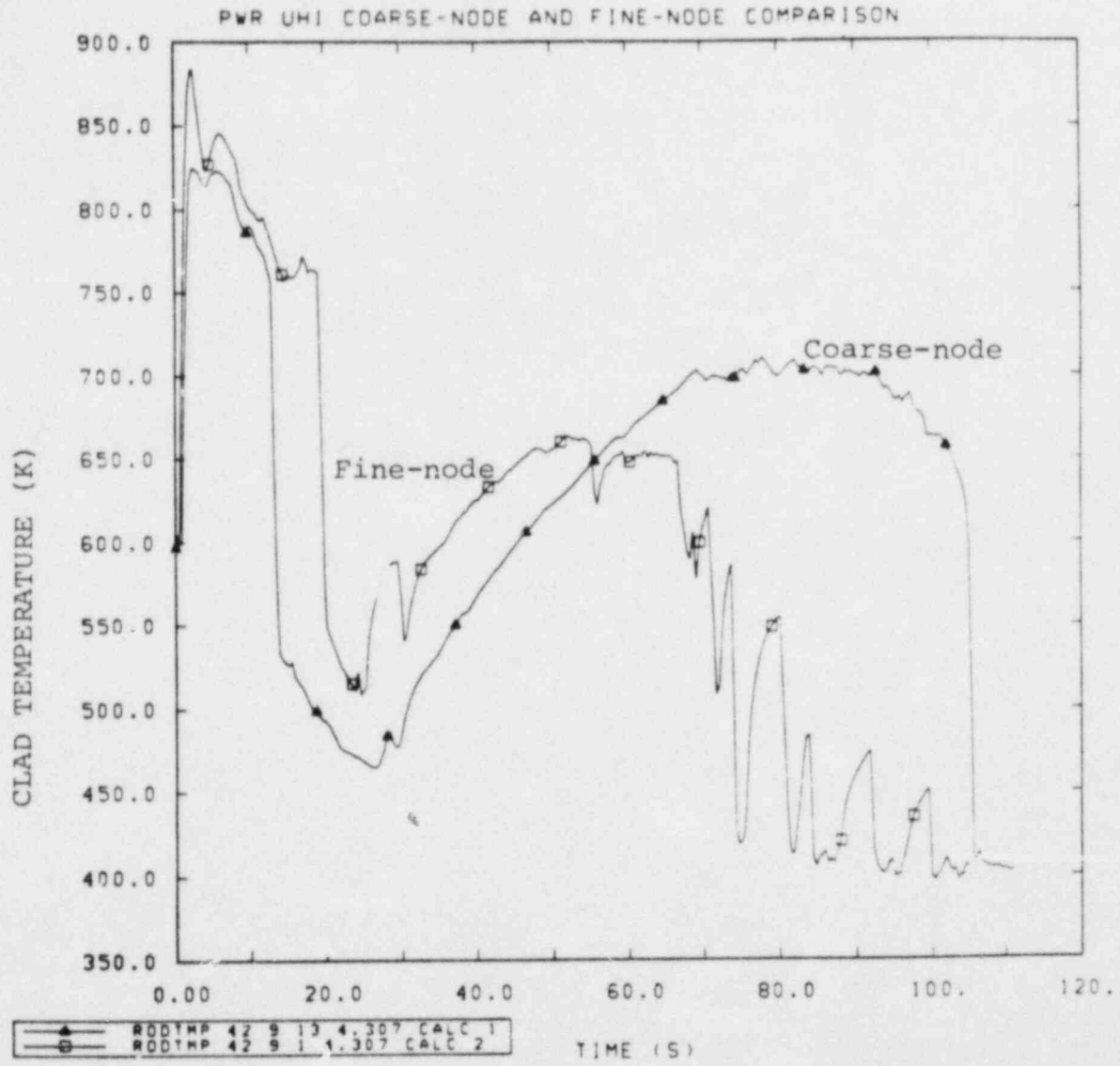PWR UHI COARSE-NODE AND FINE-NODE COMPARISON

Figure 3.14 Clad Temperature; Axial Elevation: 4.307 m,
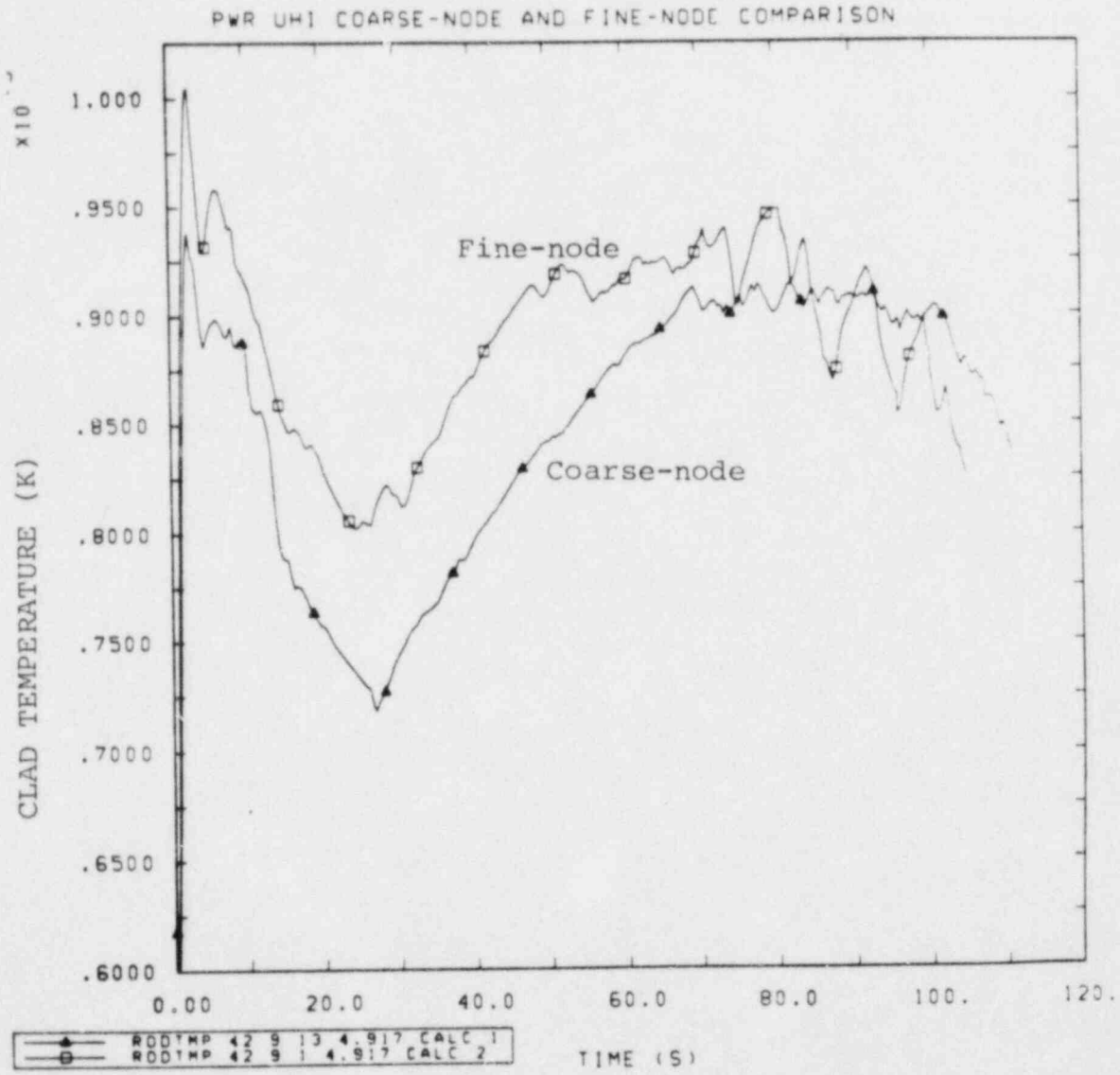Average Linear Power Generation Rate: 5.70 kW/ft

34

Figure 3.15 Clad Temperature; Axial Elevation: 4.917 m,
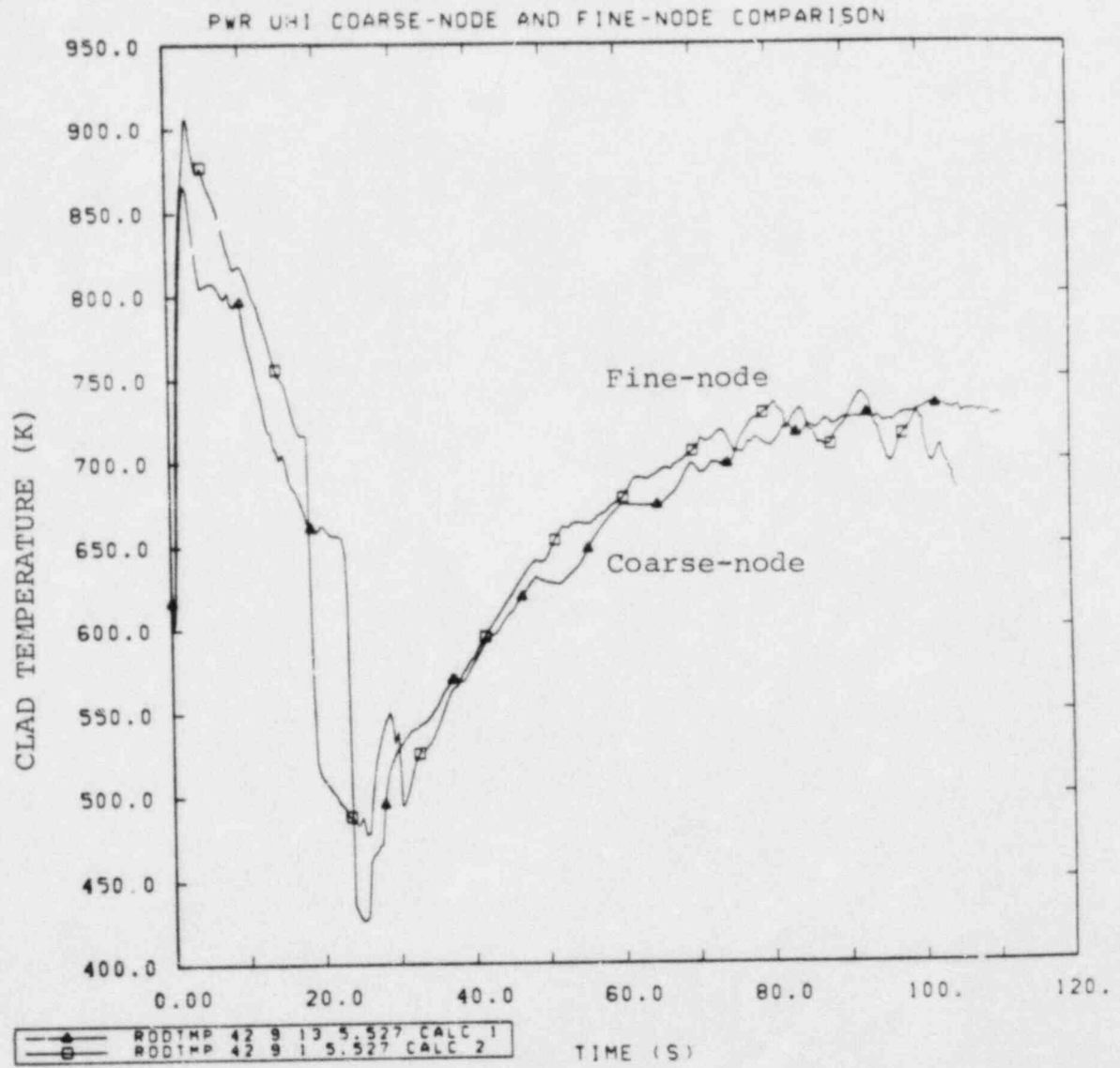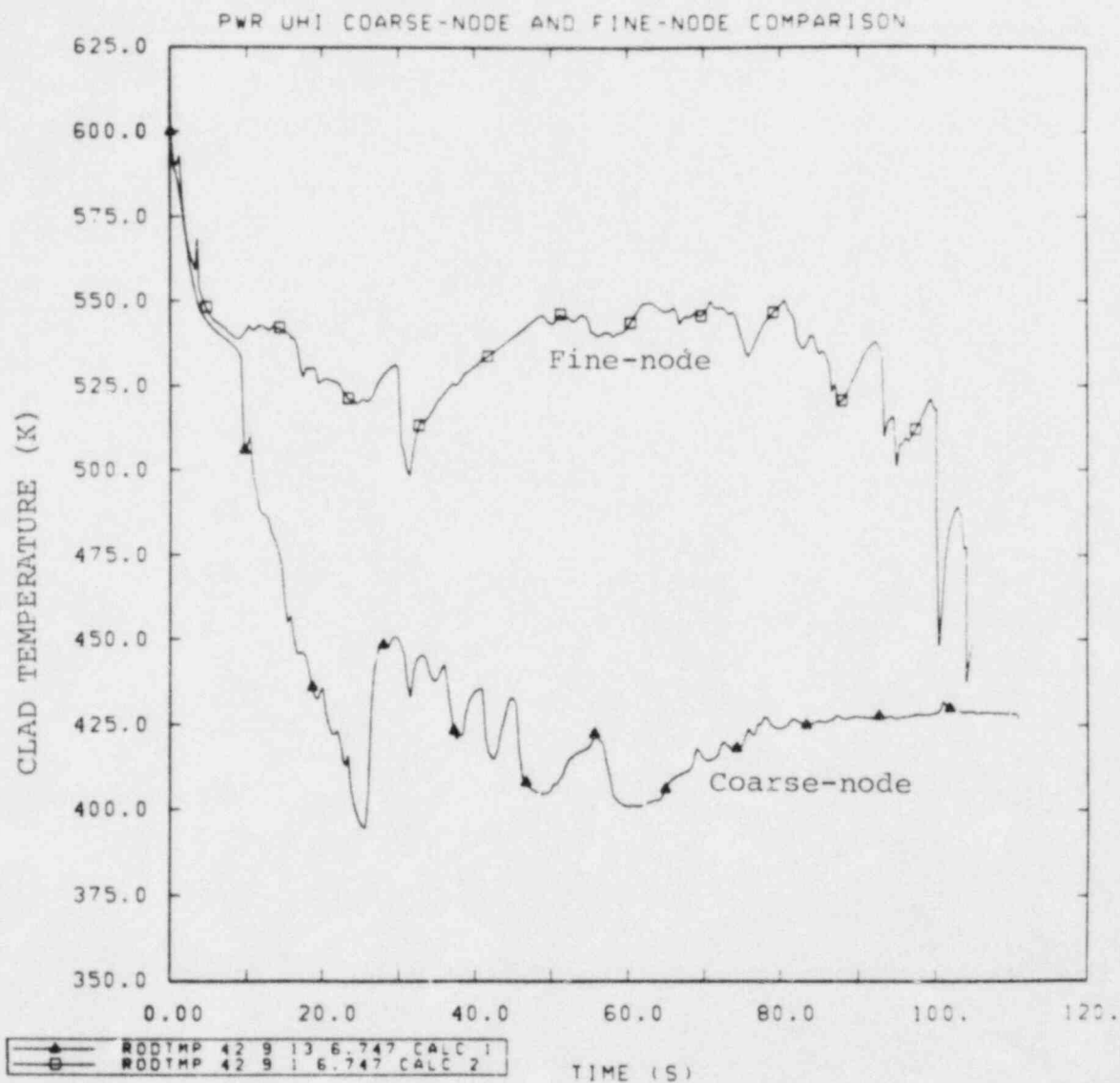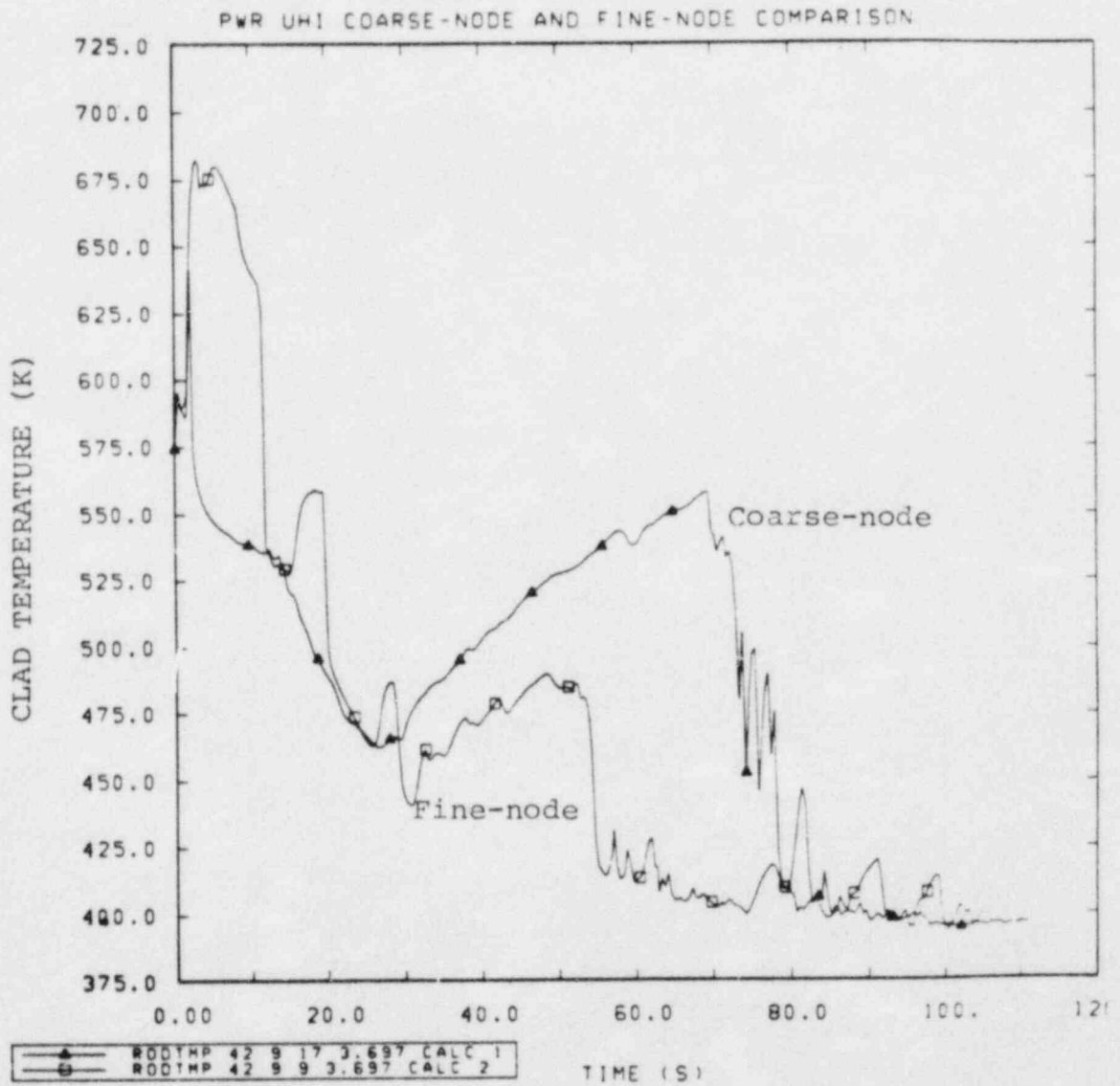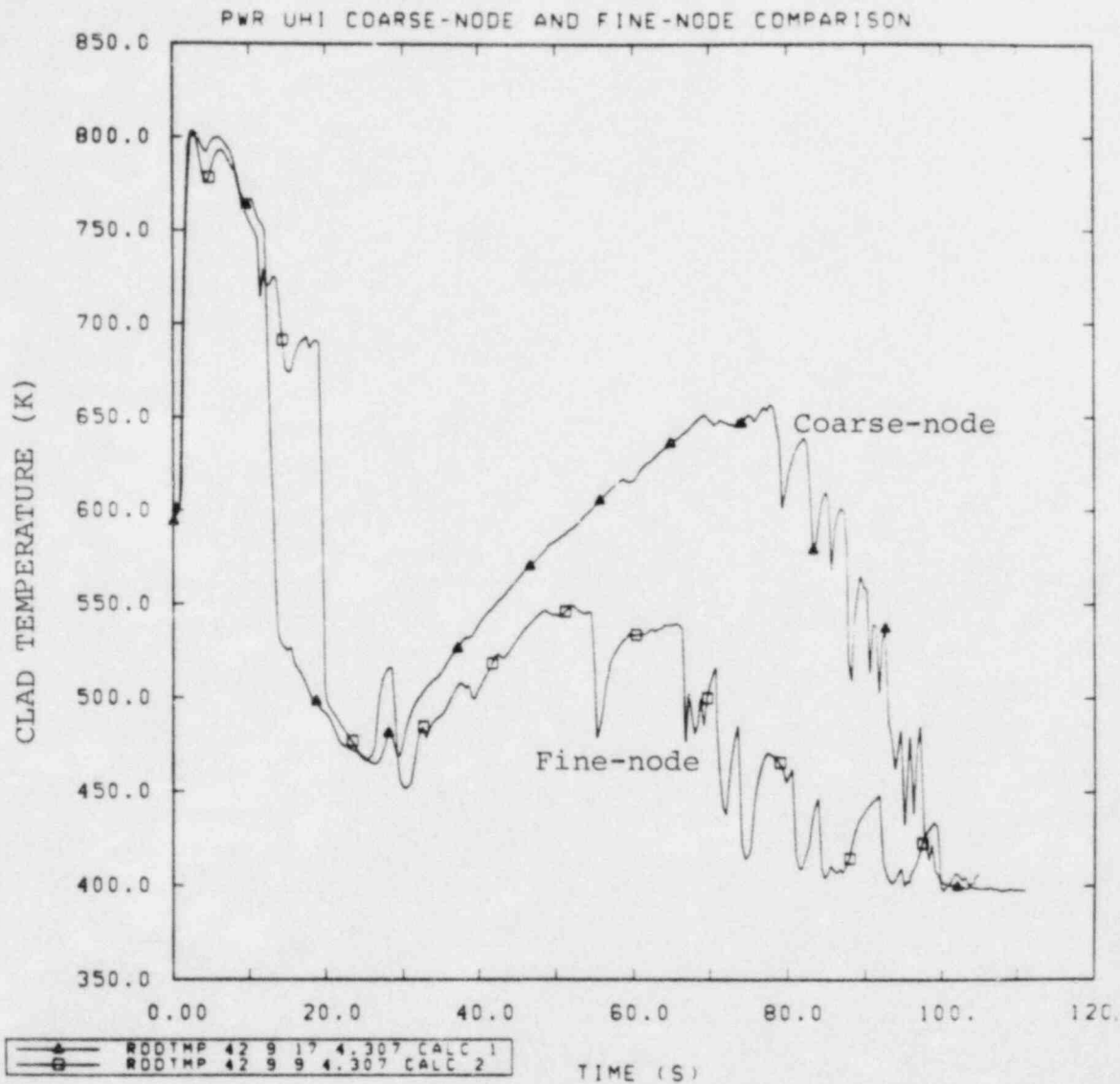Average Linear Power Generation Rate: 5.70 kW/ft

35

Figure 3.16   Clad Temperature; Axial Elevation: 5.527 m,
Average Linear Power Generation Rate: 5.70 kW/ft

Figure 3.17 Clad Temperature; Axial Elevation: 6.747 m,
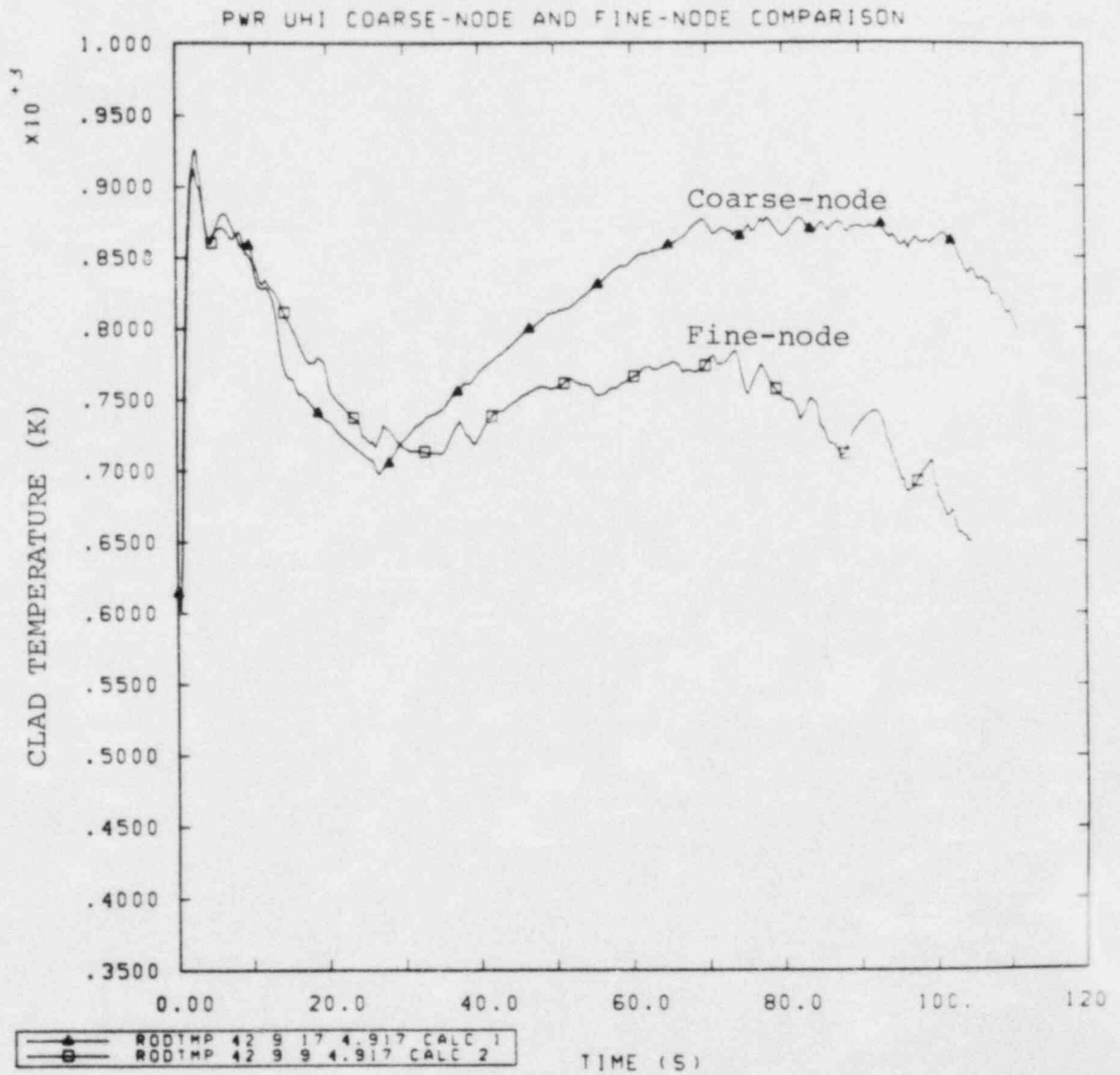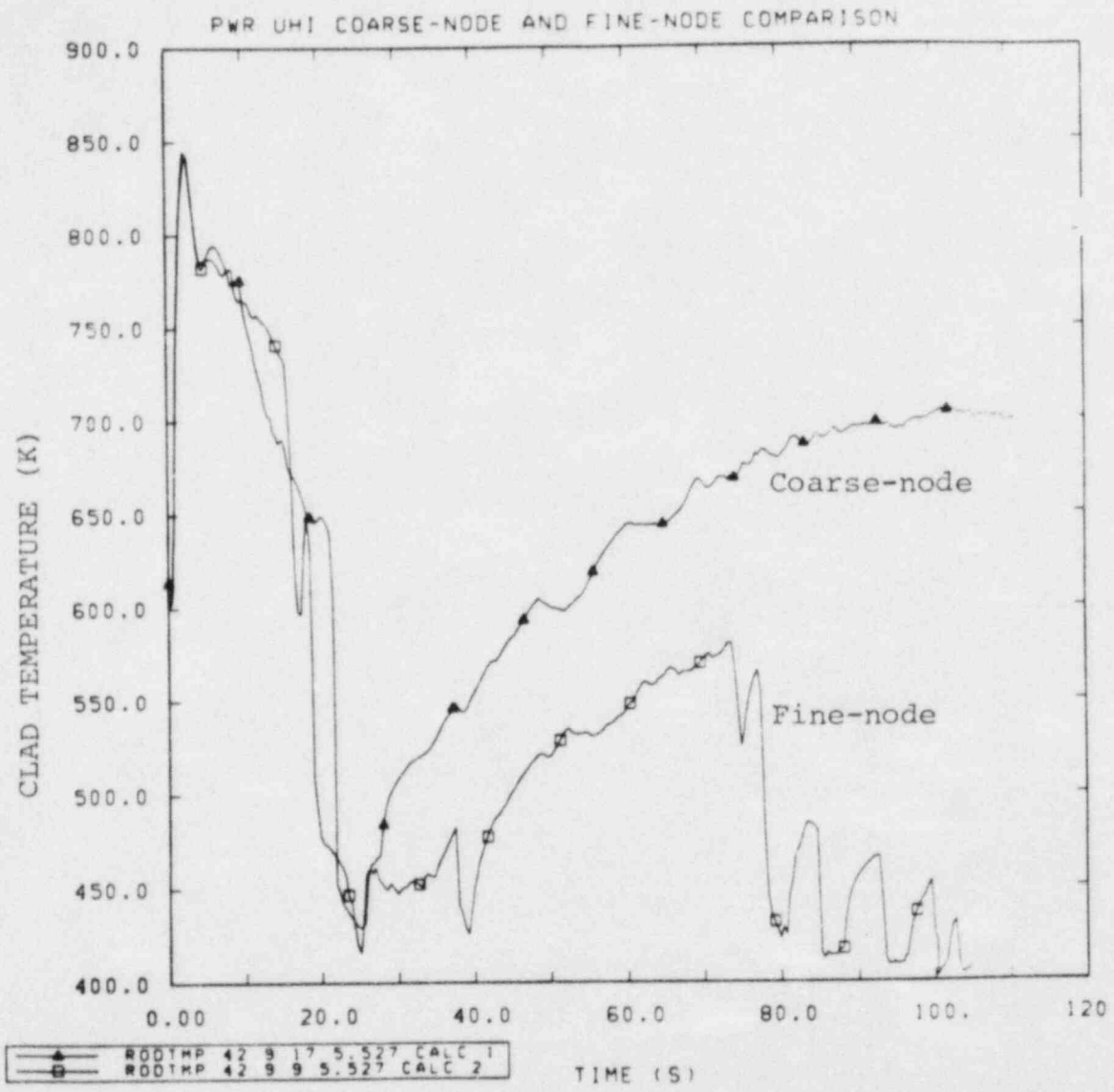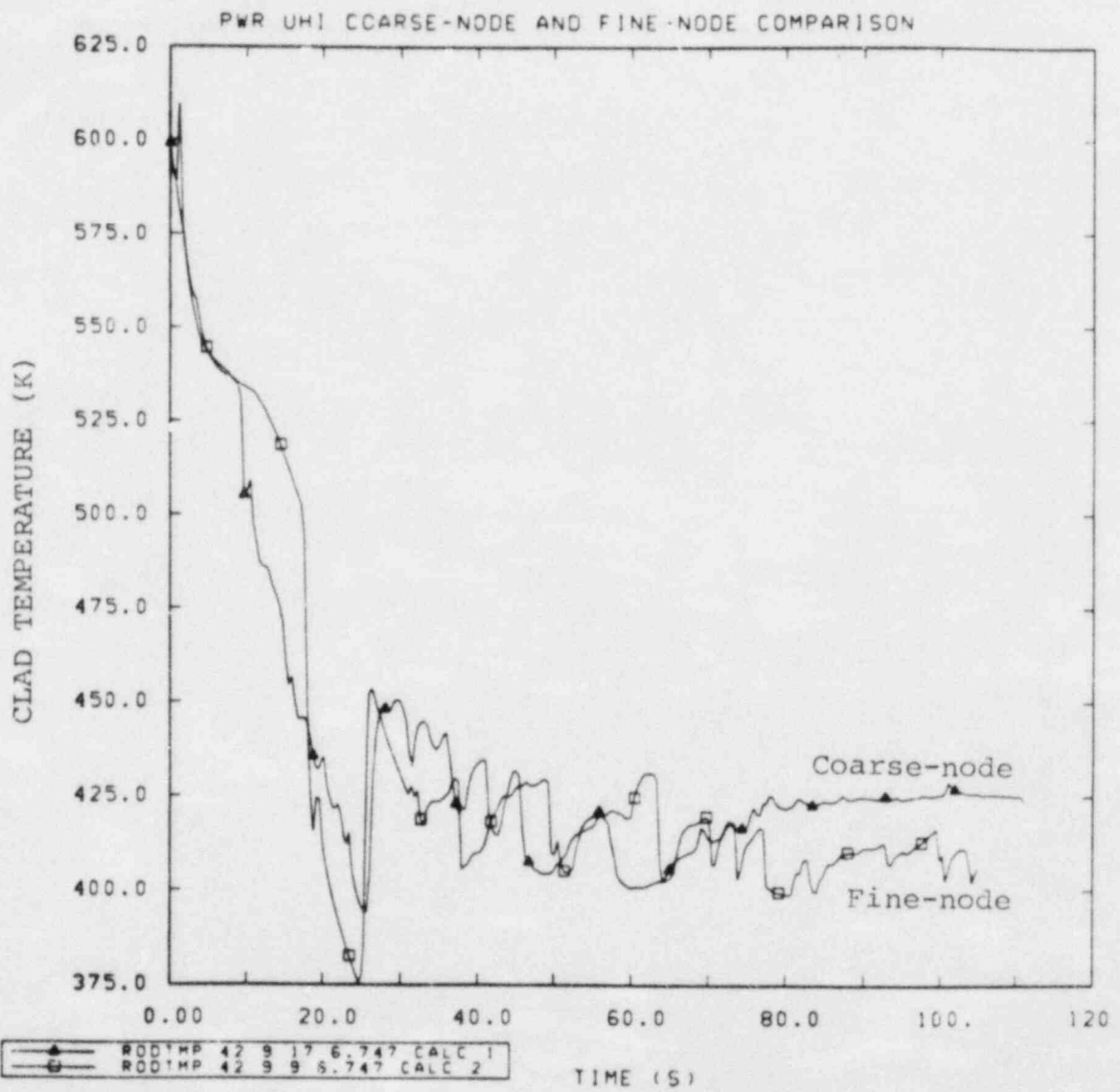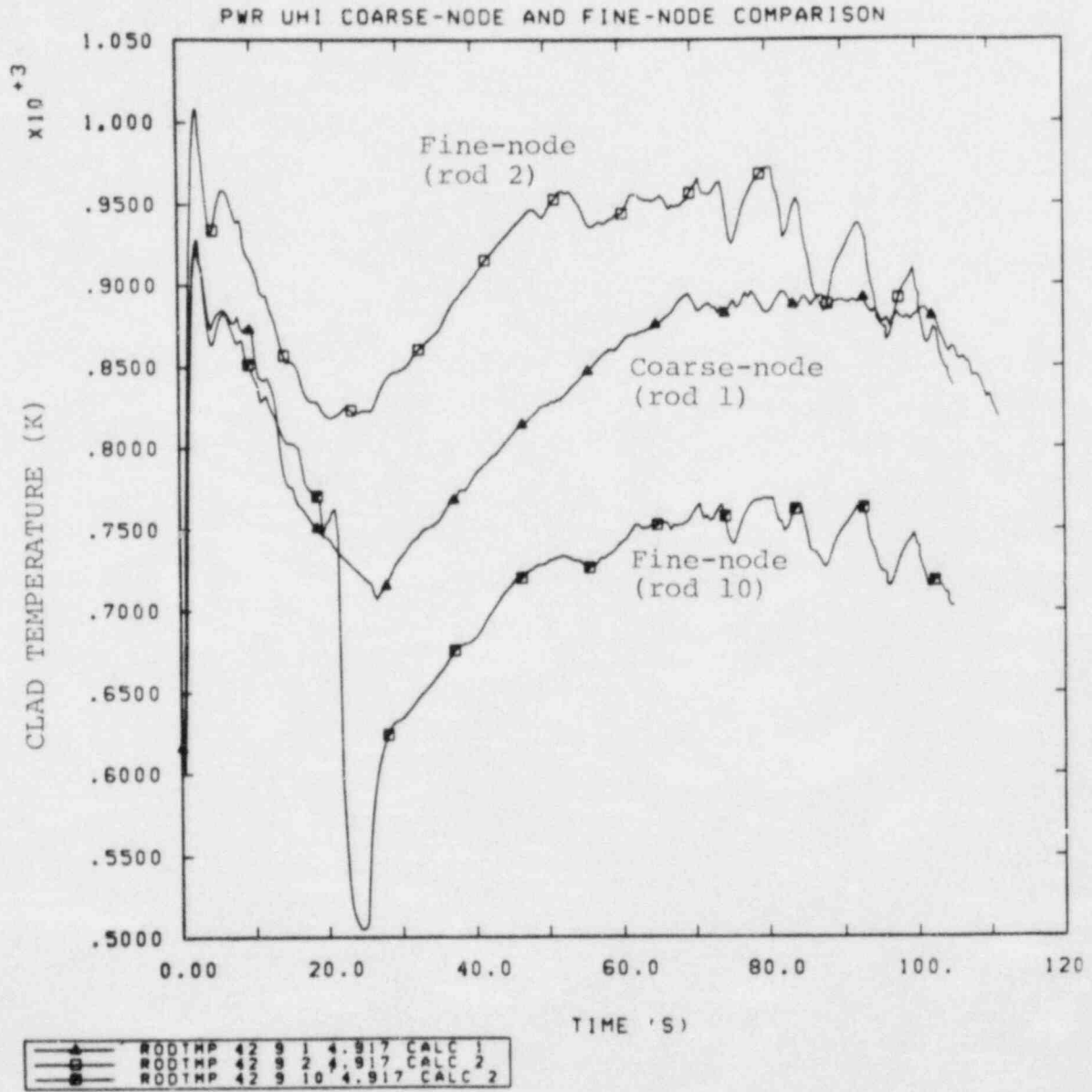Average Linear Power Generation Rate: 5.70 kW/ft

37
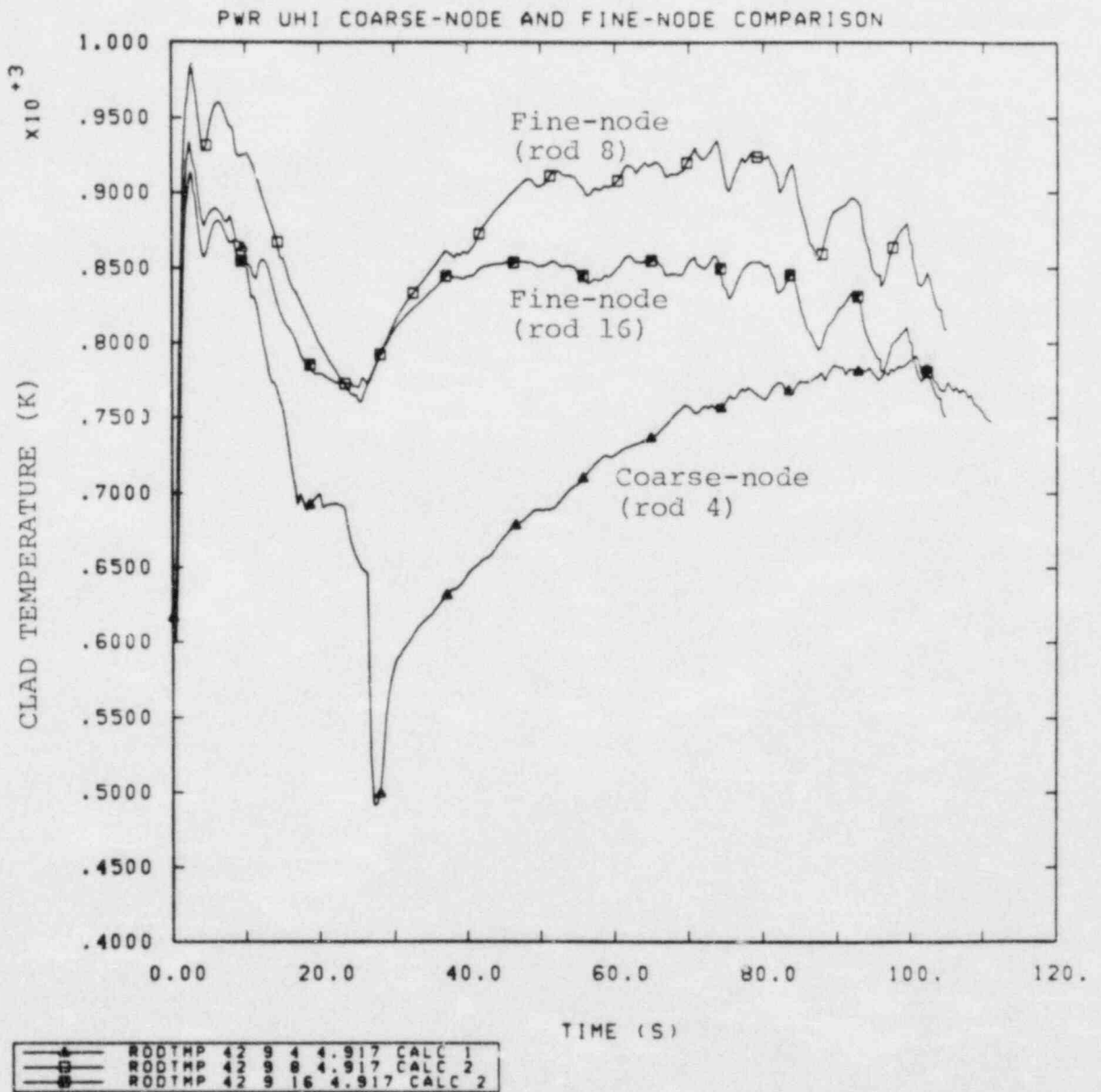
Figure 3.18   Clad Temperature at Core Midplane

Figure 3.19   Clad Temperature at Core Midplane

4.0 RELAP5/MOD1 ASSESSMENT

Most of the results from the RELAP5 assessment project were formally presented at the Eleventh Water Reactor Safety Research Information Meeting on October 27, 1983; copies of the paper prepared for the proceedings have been sent to the NRC contract monitor and to the RELAP5 code developers at INEL. More recent results from the RELAP5 assessment project were also presented at the Code Assessment Review Meeting in Denver on November 15-16, 1983.

Our RELAP5 decks for modelling the BCL ECC bypass tests were sent to INEL in December so that the RELAP5 developers could try them with a pre-release version of RELAP5/MOD2; we have not yet heard the results of their efforts.

Draft copies of the completed topical report - our RELAP5 B&W steam generator analyses were sent to the NRC contract monitor, the code developers at INEL, and B&W in early November. A draft topical report on our RELAP5/MOD1 LOFT L2-5 analyses has been completed, and copies will be sent to the NRC contract monitor and the RELAP5 code developers, probably in late January. Work continued during the quarter on preparing a topical report on the completed RELAP5/MOD1 Semiscale S-NC-3, S-NC-4 and S-NC-8 analyses.

4.1 Semiscale S-UT-8 Analysis

RELAP5/MOD1 assessment analyses of five small break experiments conducted in the Semiscale Mod-2A facility were continued into this quarter. The S-UT series of experiments investigate the effectiveness of upper head injection (UHI) of ECC during 10% and 5% communicative cold leg breaks. The initial results for the 10% and 5% breaks with and without UHI (tests S-UT-2, S-UT-1, S-UT-7, and S-UT-6, respectively) were reported in the last quarterly. [6] Analysis of an additional test, S-UT-8 [12], was performed this quarter. Test S-UT-8 was initiated from the same nominal initial conditions as test S-UT-6; however, the amount of primary coolant that bypassed the reactor vessel lower downcomer was reduced from 2.7% to 1.5% of the total flow in the loops. The decrease in the bypass flow was intended to improve the typicality of the Mod-2A system to a full-scale PWR without a UHI ECC system. The support columns installed for the Mod-2A system and used in most of the UHI tests were also blocked off for test S-UT-8 to improve the typicality; however, some instrumentation was removed from the support columns and the instrumentation ports were not plugged. This resulted in an unplanned flow path from the top of the core to the upper head during test S-UT-8.

41

A separate steady state calculation to establish the initial conditions for test S-UT-8 was performed, and Table 4.1 compares the measured initial conditions with the results of this steady state calculation. Good agreement was obtained, with the exception of the broken loop steam generator secondary pressure and broken loop pump speed. The difference in the steam generator secondary pressure occurred when the broken loop primary and secondary conditions could not be matched simultaneously. The difference in the pump speed was discussed in the last quarterly and occurs in all our Semiscale Mod-2A calculations. Since there are no reliable measurements reported for the upper head flows, the core bypass flow was set at ~1.5% of the total loop flows, based on the magnitude of the bypass flow cited in a Semiscale analysis report [13].

The calculation for test S-UT-8 was run for about 375 s of the transient. Good agreement was obtained between the calculation and some of the measurements; however, one key result was not calculated.

The predicted and observed system pressures are compared in Figure 4.1. Relatively good agreement occurred during the initial 25 s of the transient; however, after 25 s the calculated primary pressure was higher than that measured. The primary cause of the higher calculated primary pressure was the prediction of a higher steam generator secondary pressure than was measured. Figure 4.2 compares the calculated and measured intact loop primary and steam generator secondary pressures, and shows that the calculated peak secondary pressure was about 0.5 MPa higher than measured. The higher calculated steam generator pressure resulted in higher calculated fluid temperatures on the secondary side of the steam generator than were observed, as shown in Figure 4.3. The higher fluid temperatures in turn resulted in less energy being removed from the primary system in the calculation.

Good overall agreement was obtained between the calculated and measured break mass flow as indicated in Figure 4.4. When we stopped the calculation, the measured and calculated total mass flows out of the primary system agreed to within ~1 kg.

The calculated and measured intact loop hot leg densities are shown in Figure 4.5. The measured results include a top and a body densitometer measurement. The measurements indicate the fluid was stratified very early in the transient. A comparison of the calculated and measured results indicates the hot leg drained at about 125 s in the calculation, whereas, in the test, liquid remained on the bottom of the pipe until 650 s when the hot leg drained.

A significant event during test S-UT-8 was the depression of the core liquid level down to the core inlet elevation at ~215 s. This level depression appeared to be caused by primary system liquid remaining in the upflow leg of the intact loop steam generator U-tubes after the downflow leg had cleared and before the intact loop pump suction downflow leg had cleared. The primary system fluid in the upflow side of the steam generator tubes exerted a pressure head on the vessel liquid and depressed the level below the core inlet. [13]

Calculated and measured densities 2.53 m and 1.73 m above the core inlet are shown in Figures 4.6 and 4.7, respectively. The measured liquid level dropped below the 2.53 m core elevation at ~160 s and recovered at 260 s, as shown by the measured density in Figure 4.6. The calculated liquid level, indicated by the density at the 2.53 m core elevation, dropped below this elevation at about 195 s and recovered a few seconds later. The measured level dropped below the 1.73 m core elevation as shown by the measured density in Figure 4.7. The calculated level did not drop below the 1.73 m core elevation. In the test, the core liquid level dropped below the core inlet, whereas the calculated level only dropped to the 2.53 m core elevation.

The drop in the core liquid level in the test resulted in a temperature increase at the lower core elevations. Calculated and measured rod cladding temperature at the 1.5 to 1.8 m core elevation are compared in Figure 4.8. (The initial difference in the temperatures is due to the measured temperature being from an embedded thermocouple and the calculated temperature being at the rod surface. Later in the transient this difference in location is not significant.) Figure 4.8 shows that the measured temperature increased to ~680 K at 225 s, while the calculated rod temperature remained near the system saturation temperature. Figure 4.8 also shows that a rod heatup was measured later in the transient. The calculation has not been run far enough to determine if the later rod heatup would be calculated. We anticipate that the later rod heatup would be calculated, since a heatup was calculated for Test S-UT-6. [6]

The primary reason that the level did not drop as far in the calculation as occurred in the test was that primary liquid did not accumulate in the upflow side of the intact loop steam generator tubes after the downflow side of the tubes had cleared of liquid. The measured and calculated collapsed liquid levels in the primary side of the intact loop steam generator are compared in Figure 4.9. The calculated collapsed liquid level in both the upflow side and the downflow side cleared much earlier in the calculation than in the test. The probable cause of the earlier clearing is that the energy transfer from the primary system to the steam generators was too low in the calculation. The calculation of higher secondary pressures than measured would contribute to this result.

43

To determine if the calculation of the steam generator pressure was the major contributor to the difference between the calculated and measured results, the calculation was repeated with the measured pressure in the intact and broken loop steam generators input to the calculation. Figure 4.10 compares calculated and measured primary system pressures, and shows improved agreement between the calculation and the measurement. This result shows that the conditions in the steam generators had a significant effect on the calculated primary pressure. The calculation using the steam generator pressure as input increased the time before the upflow side of the tubes cleared by ~10 s, but this did not have a significant effect on the core collapsed liquid level.

In summary, not calculating the correct steam generator secondary response resulted in differences between the measured and calculated primary system pressures. The early depression of the core liquid level down to the core inlet was not calculated. The reason appears to be that, in the analysis, primary liquid did not accumulate in the upflow side of the steam generator tubes. Using the steam generator secondary pressure as input to the calculation improved the agreement with the primary system pressure but did not result in the calculation of the early core level depression. The results of these calculations are still being analyzed, and preparation of a topical report on our S-UT analyses has begun.

Table 4.1 Measured and Calculated Initial Conditions for Test S-UT-8

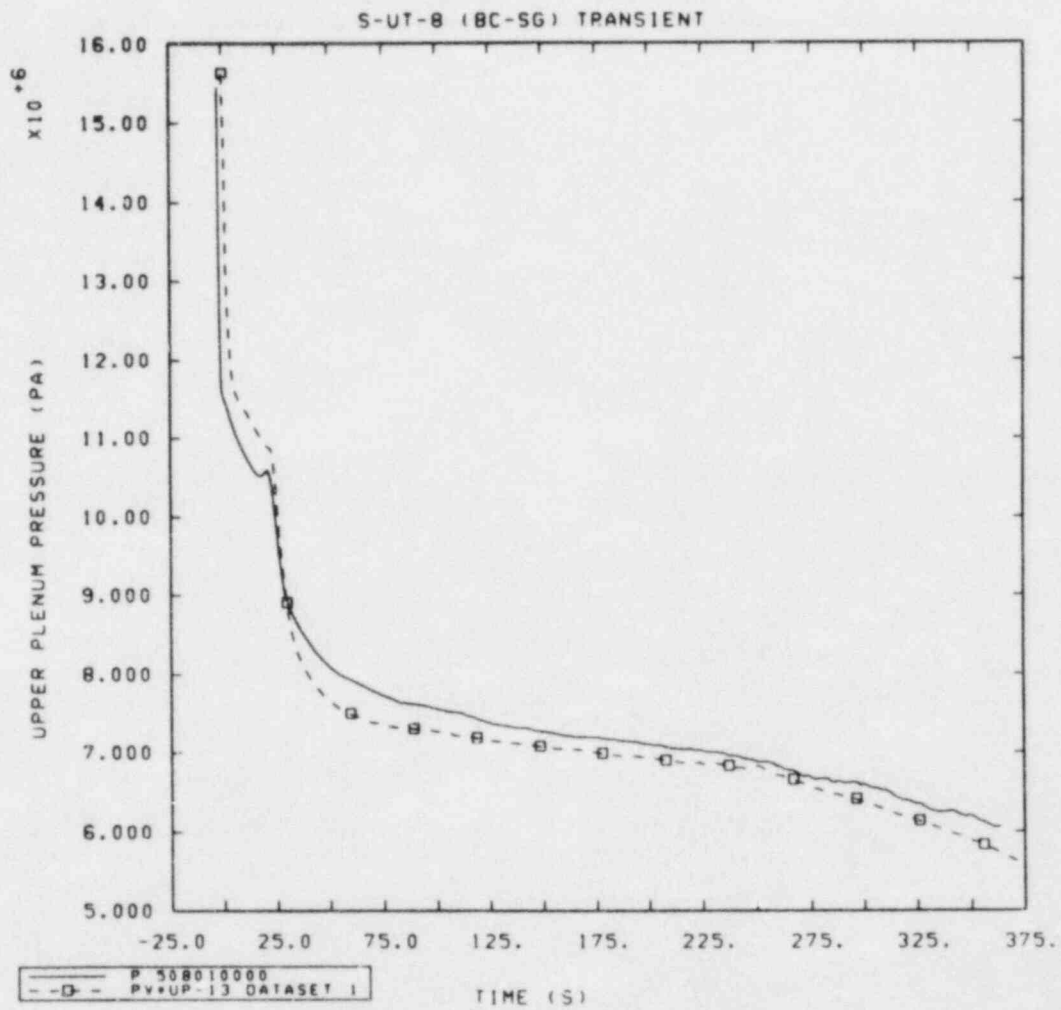|	S-UT-8	RELAP5
Core Power (MW)	1.95	1.95
System Pressure (MPa)	15.6	15.5
IL Cold Leg Temperature (K)	559.5	559.5
IL Core Temperature Rise (K)	35.1	35.2
IL Cold Leg Flow (ℓ/s)	10.3	9.9
IL Steam Generator Pressure (MPa)	5.71	5.75
IL Pump Speed (rad/s)	244	226
BL Cold Leg Temperature (K)	561.4	561.4
BL Core Temperature Rise (K)	33.8	33.3
BL Cold Leg Flow (ℓ/s)	3.3	3.3
BL Steam Generator Pressure (MPa)	6.11	6.00
BL Pump Speed (rad/s)	1192	1486
Bypass Flow (ℓ/s)	NM*	0.22**
Support Column Flow (ℓ/s)	NM*	0.12

* Not measured
** Set at ~1.5% of total loop flow

44

Figure 4.1 Calculated and Measured Primary System
Pressure for test S-UT-8

45

S-UT-8 (BC-SG) TRANSIENT

PRESSURE (PA) ×10⁺⁶

16.00
15.00
14.00
13.00
12.00
11.00
10.00
9.000
8.000
7.000
6.000
5.000

0.00   50.0   100.   150.   200.   250.   300.   350.

TIME (S)

P 508010000
P 204010000
PV*UP-13 DATASET 1
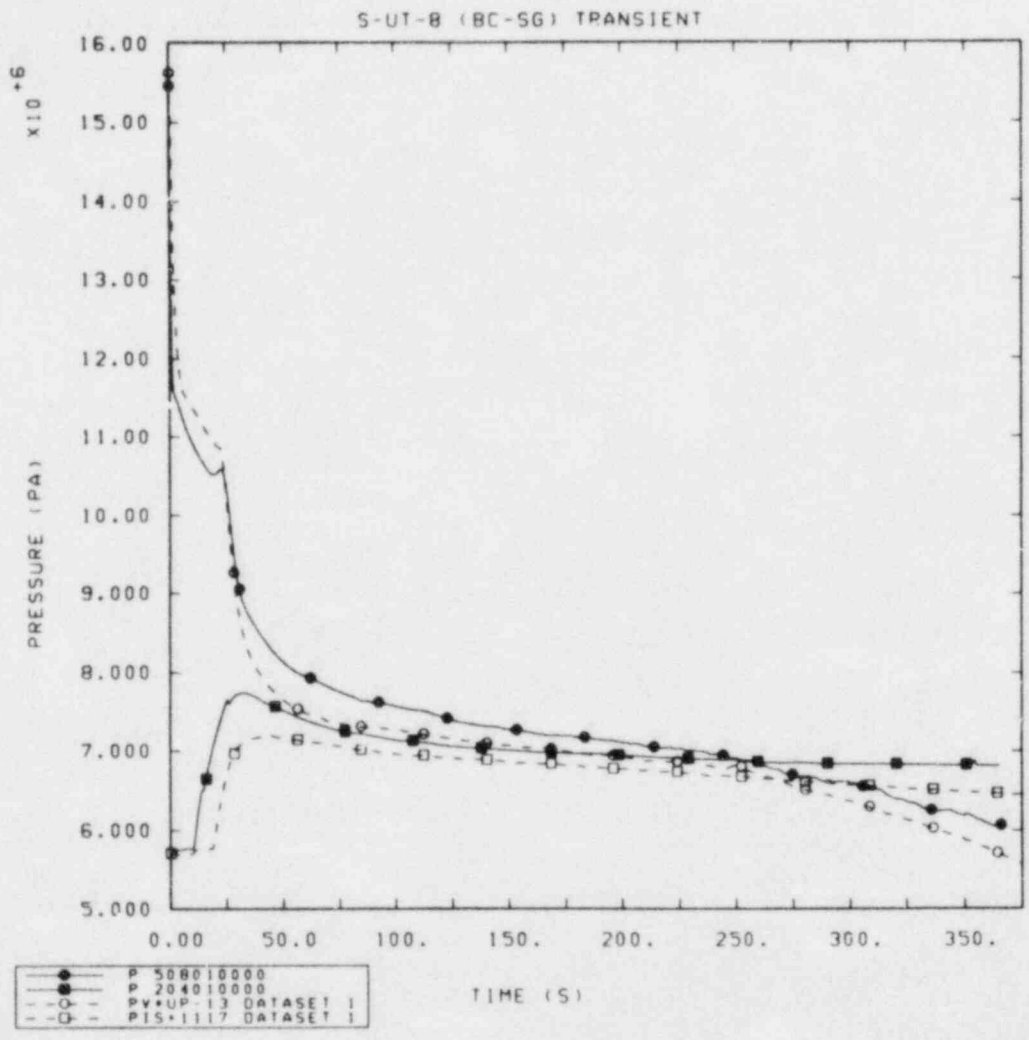PIS*1117 DATASET 1

Figure 4.2   Calculated and Measured Primary System
and Intact Loop Steam Generator Secondary
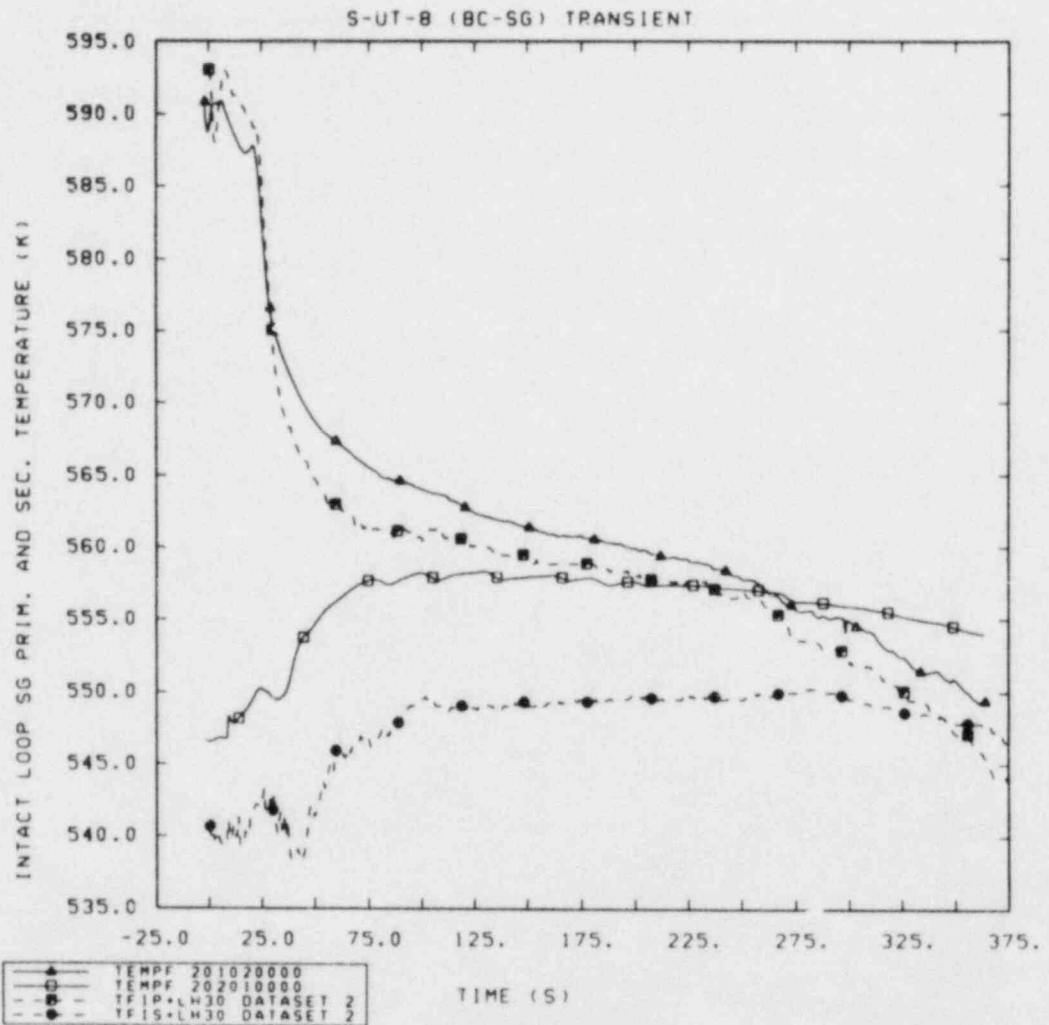Pressure for test S-UT-8

46

Figure 4.3   Calculated and Measured Intact Loop Steam
Generator Secondary Fluid Temperature for
test S-UT-8
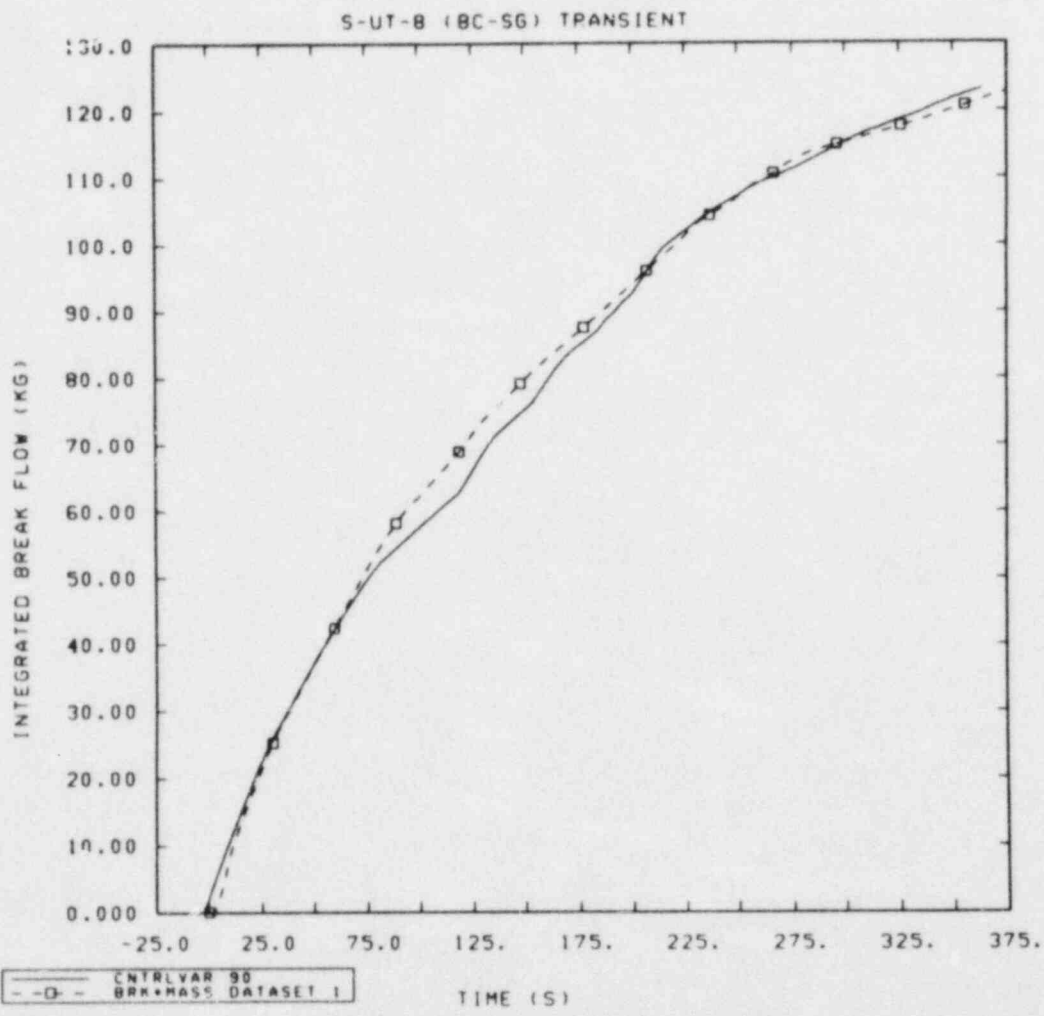
47

Figure 4.4   Calculated and Measured Total Break Mass
             Flow for test S-UT-8

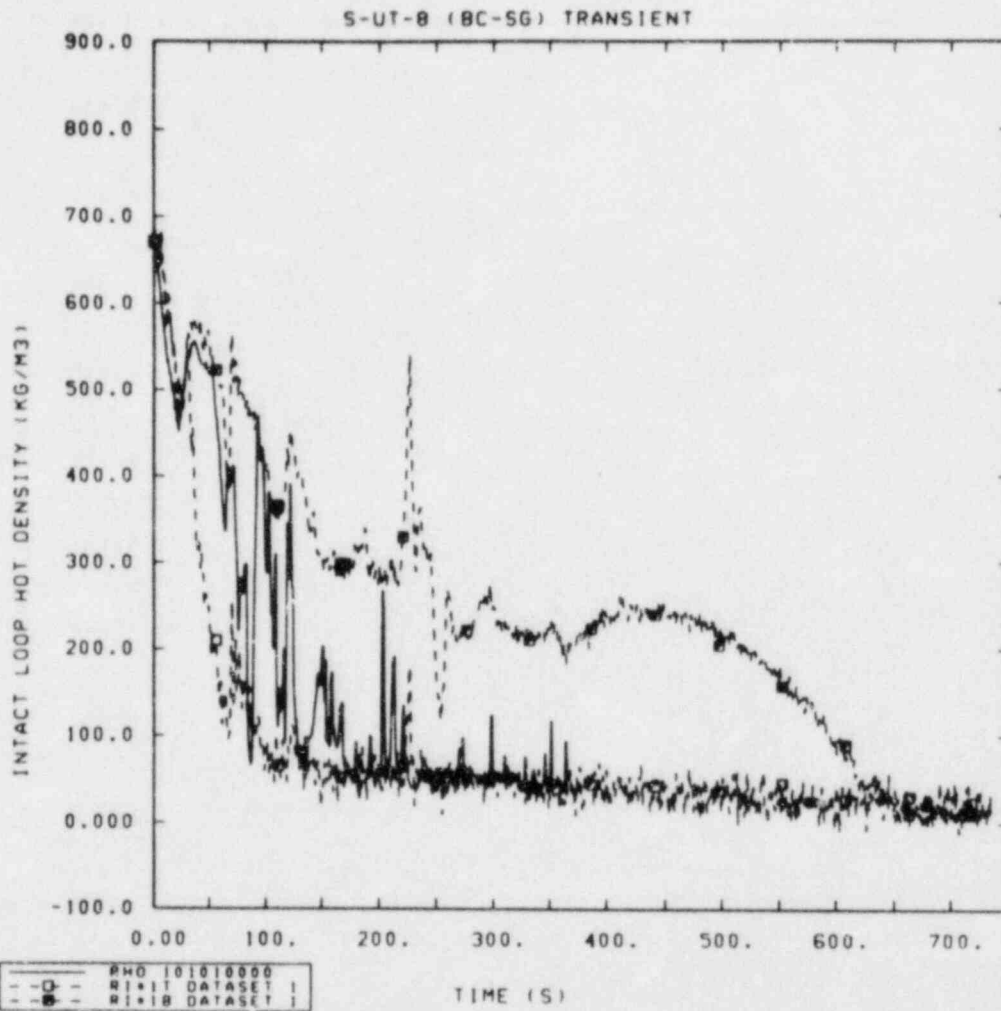Figure 4.5   Calculated and Measured Intact Loop
Hot Leg Density for test S-UT-8
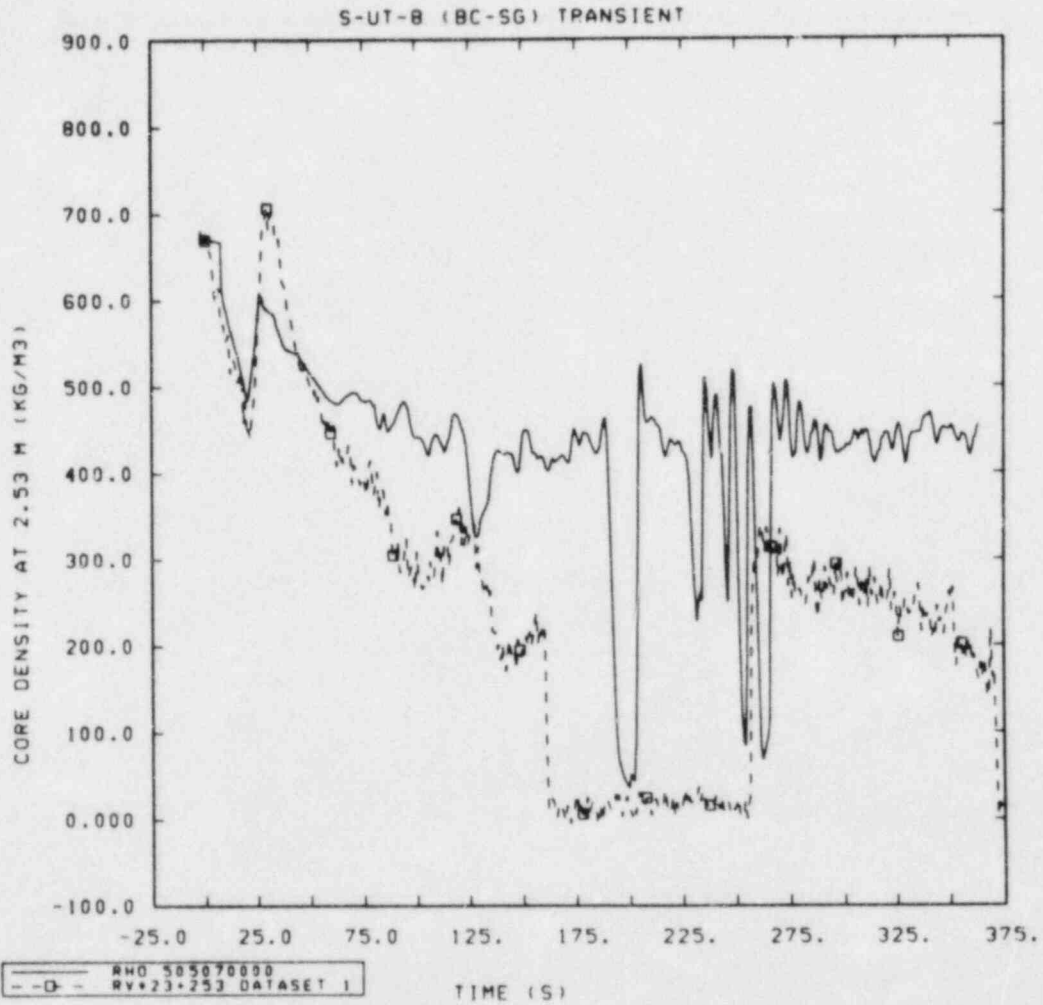
Figure 4.6   Calculated and Measured Density at the
2.53 m Core Elevation for test S-UT-8

50
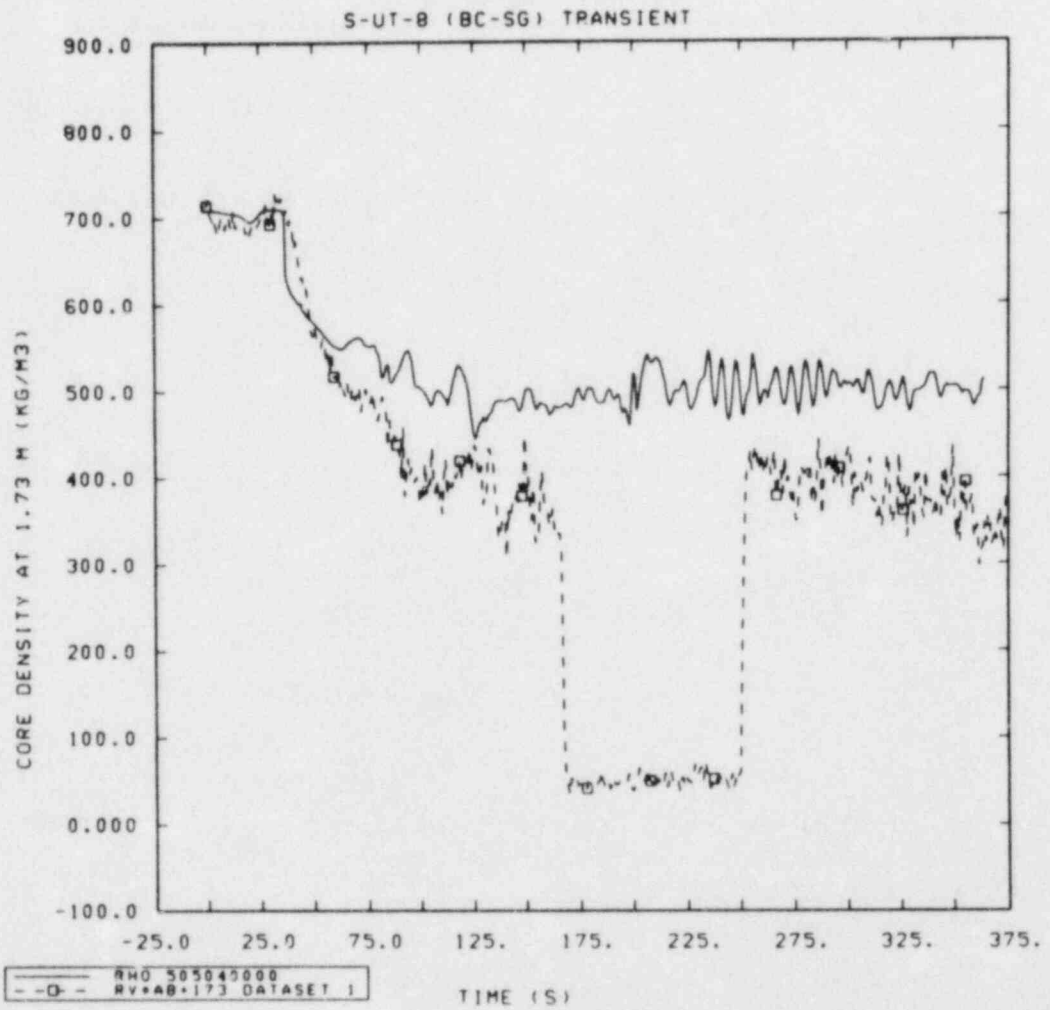
Figure 4.7 Calculated and Measured Density at the
1.73 m Core Elevation for test S-UT-8

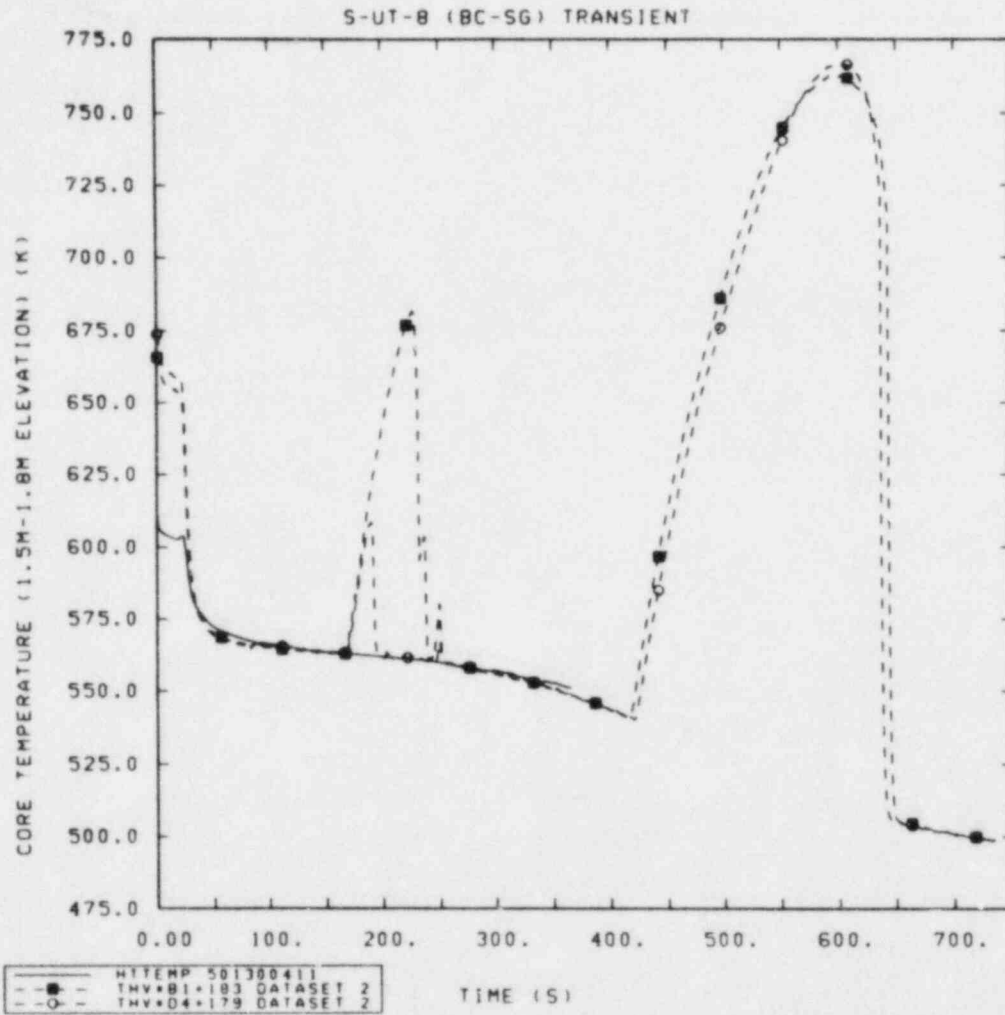Figure 4.8   Calculated and Measured Rod Cladding
            Temperature at the 1.5 m-1.8 m Core
            Elevation for test S-UT-8
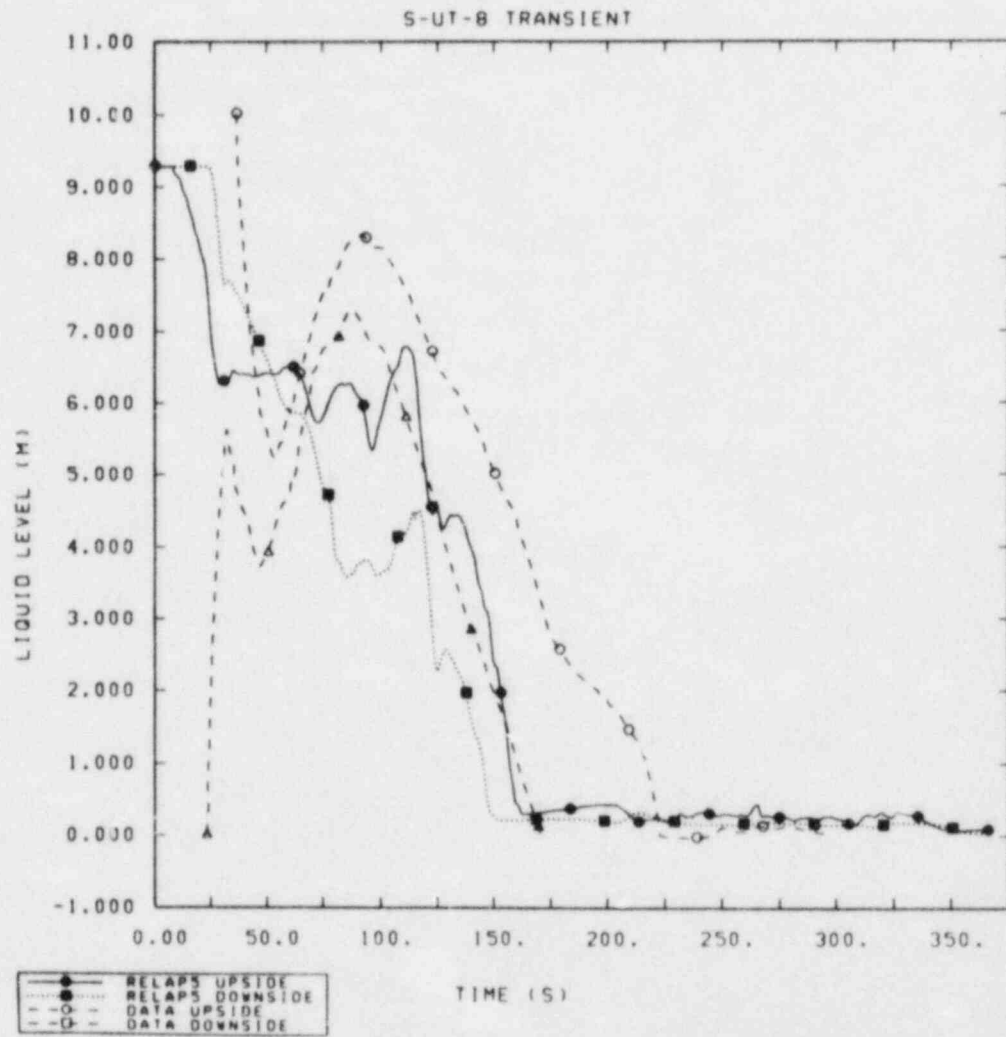
Figure 4.9   Calculated and Measured Intact Loop
              Steam Generator Primary Side Collapsed
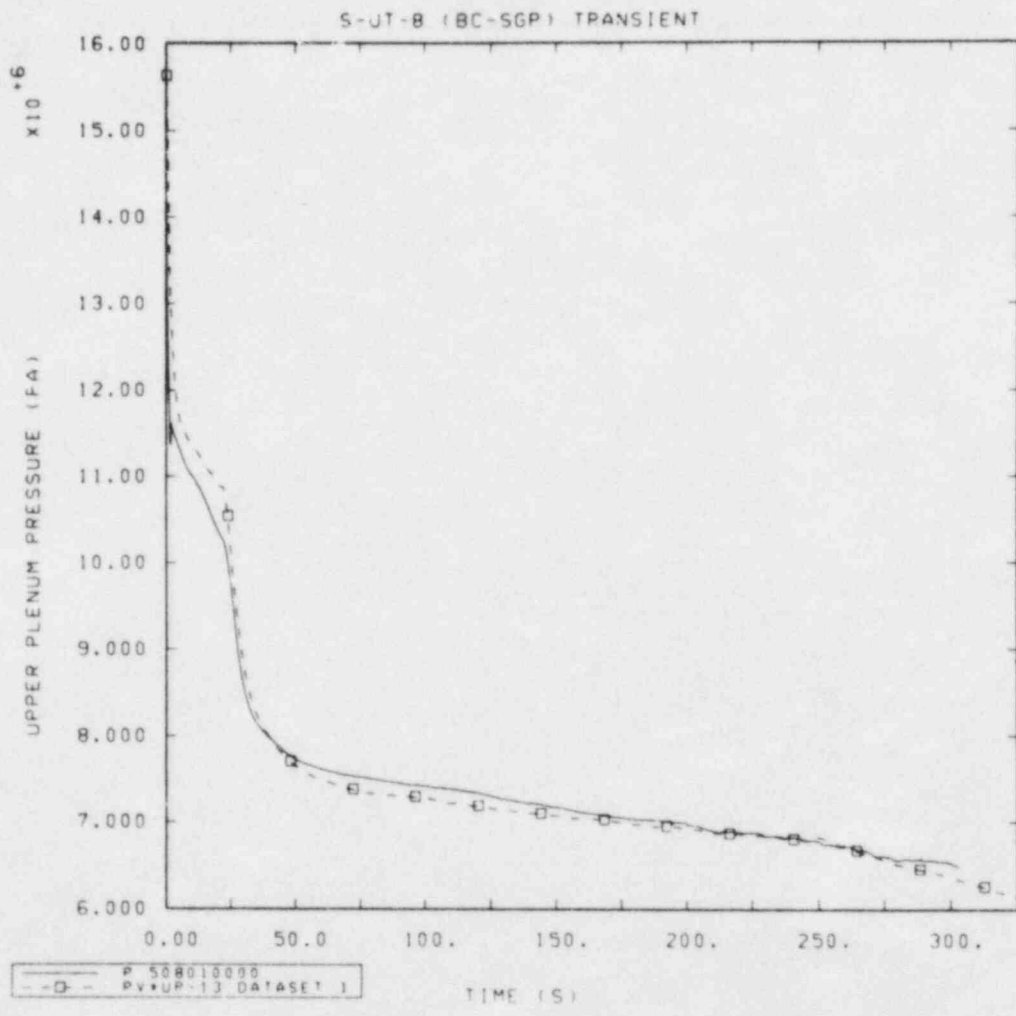   Liquid Level for test S-UT-8

53

Figure 4.10   Calculated (using steam generator
pressures as input) and Measured Primary
System Pressure for test S-UT-8

5.0 REFERENCES

1. TRAC-PF1/MOD1: An Advanced Best-Estimate Computer Program
    for Pressurized Water Reactor Thermal-Hydraulic Analysis
    (Draft), Safety Code Development Group, Energy Division, Los
    Alamos National Laboratory, 1983.

2. L. D. Buxton, TRAC-PF1 Analysis of a Large Break LOCA for a
    UHI Plant, letter report to N. Lauben, NRC, Sandia National
    Laboratories, February 10, 1983.

3. D. Dobranich, L. D. Buxton and C. C. Wong, TRAC-PF1
    Independent Assessment: TRAC-PF1 Noding Study, to be
    published.

4. A. C. Peterson, RELAP5 Assessment: Semiscale Mod-2A S-UT
    Small Break Tests, Sandia National Laboratories, to be
    published.

5. S. L. Thompson et al., Thermal/Hydraulic Analysis Research
    Program Quarterly Report, April-June 1983, NUREG/CR-3329
    (Vol. 2 of 4), SAND83-1171, Sandia National Laboratories,
    September 1983.

6. S. L. Thompson et al., Thermal/Hydraulic Analysis Research
    Program Quarterly Report, July-September 1983, NUREG/CR-3329
    (Vol. 3 of 4), SAND83-1171, Sandia National Laboratories,
    December 1983.

7. B. Brand, R. Kirmse and W. Winkler, OECD-CSNI Standard
    Problem No. 10: Refill and Reflood Experiments in a
    Simulated PWR Primary System (PKL), GRS report, December
    1979.

8. D. Hein et al, PKL-Small Breaks (Test Series ID): Results of
    the Steady-State Test PKL ID1 in a Four-Loop Operation with
    30 Bar System Pressure, KWU Tech. Rept. No. R 513/18/81,
    April 1981.

9. S. L. Thompson and L. N. Kmetyk, RELAP5 Assessment: PKL
    Natural Circulation Tests, NUREG/CR-3100, SAND82-2902,
    Sandia National Laboratories, January 1983.

10. H. R. Carter and D. D. Schleappi, Nuclear Once-Through Steam
    Generator (OTSG and IEOTSG) Loss of Feedwater Flow (LOFW)
    Test, Report No. 4707, Babcock & Wilcox Co., March 1978.

11. R. M. Summers, RELAP5 Assessment: B&W 19-Tube Once-Through
    Steam Generator (OTSG) Loss of Feedwater Test,
    NUREG/CR-3302P, SAND83-2169, Sandia National Laboratories,
    December 1983.

12. W. W. Tingle, <u>Experiment Operating Specification for Semiscale Mod-2A 5% Break Experiment S-UT-8</u>, EGG-SEMI-5865, Idaho National Engineering Laboratory, December 1981.

13. M. T. Leonard, <u>Vessel Coolant Mass Depletion during a Small Break LOCA</u>, EGG-SEMI-6013, Idaho National Engineering Laboratory, September 1982.

DISTRIBUTION: Thermal/Hydraulic Analysis Research Program
Quarterly Report October-December 1983

U. S. NRC Distribution Contractor (CDSI) (300)
7300 Pearl Street
Bethesda, MD 20014
        300 copies for R4

U. S. Nuclear Regulatory Commission (4)
Reactor Systems Research Branch
Division of Accident Evaluation
Office of Nuclear Regulatory Research
7915 Eastern Avenue
Silver Spring, MD 20910
Attn: Louis M. Shotkin
      Fuat Odar
      P. Landry
      H. S. Tovmassian

EG&G Idaho (6)
Idaho National Engineering Laboratory
P. O. Box 1625
Idaho Falls, ID 83415
Attn: T. R. Charlton
      G. W. Johnsen
      Edna Johnson
      J. C. Lin
      V. H. Ransom
      R. J. Wagner

Thad D. Knight
Dennis R. Liles
Los Alamos National Laboratory (2)
K553 Q-9
Los Alamos, NM 87545

P. Saha, 130
Department of Nuclear Energy
Brookhaven National Laboratory
Associated Universities, Inc.
Upton, New York 11973

N. H. Shah
Babcock & Wilcox Co. (NPGD)
P. O. Box 1260
Lynchburg, VA 24505

Jesse Fell (5)
Deputy Director, Water Reactor Programs
Atomic Energy Establishment
Winfrith
Dorchester, Dorset DT28DH
ENGLAND

6400 A. W. Snyder
6410 J. W. Hickman
6417 D. C. Carlson
6420 J. V. Walker
6421 T. R. Schmidt
6422 D. A. Powers
6423 P. S. Pickard
6425 W. J. Camp
6427 M. Berman
6427 C. C. Wong
6440 D. A. Dahlgren
6442 W. A. von Riesemann
6444 S. L. Thompson (15)
6444 L. D. Buxton
6444 R. K. Byers
6444 R. K. Cole, Jr.
6444 P. N. Demmie
6444 D. Dobranich
6444 M. G. Elrick
6444 L. N. Kmetyk
6444 R. Knight
6444 J. M. McGlaun
6444 J. Orman
6444 A. C. Peterson
6444 W. R. Schmidt
6444 R. M. Summers
6444 S. W. Webb
6444 G. G. Weigand
6449 K. D. Bergeron
3141 C. M. Ostrander (5)
3151 W. L. Garner
8424 M. A. Pound

BIBLIOGRAPHIC DATA SHEET

1. REPORT NUMBER (Assigned by TIDC add Vol. No. if any)
NUREG/CR-3329 Vol. 4 of 4
SAND83-1171

2. Leave blank

3. TITLE AND SUBTITLE
Thermal/Hydraulic Analysis Research Program Quarterly Report October-December 1983

4. RECIPIENT'S ACCESSION NUMBER

5. DATE REPORT COMPLETED	
MONTH	YEAR
February	1984

6. AUTHOR(S)
S. L. Thompson, Person in Charge

7. DATE REPORT ISSUED	
MONTH	YEAR
March	1984

8. PERFORMING ORGANIZATION NAME AND MAILING ADDRESS (Include Zip Code)
Sandia National Laboratories
Thermal/Hydraulic Analysis Division 6444
P. O. Box 5800
Albuquerque, NM 87185

9. PROJECT/TASK/WORK UNIT NUMBER

10. FIN NUMBER (S)
A-1205 & A-1374

11. SPONSORING ORGANIZATION NAME AND MAILING ADDRESS (Include Zip Code)
Reactor Systems Research Branch
Division of Accident Evaluation
Office of Nuclear Regulatory Research
U. S. Nuclear Regulatory Commission
Washington, DC 20555

12a. TYPE OF REPORT
Technical

12b. PERIOD COVERED (Inclusive dates)
October-December 1983

13. SUPPLEMENTARY NOTES

14. ABSTRACT (200 words or less)

15a. KEY WORDS AND DOCUMENT ANALYSIS	15b. DESCRIPTORS

16. AVAILABILITY STATEMENT	17. SECURITY CLASSIFICATION (This report)	18. NUMBER OF PAGES
	Uncl	63
	19. SECURITY CLASSIFICATION (This page)	20. PRICE
	Uncl	$

-59-